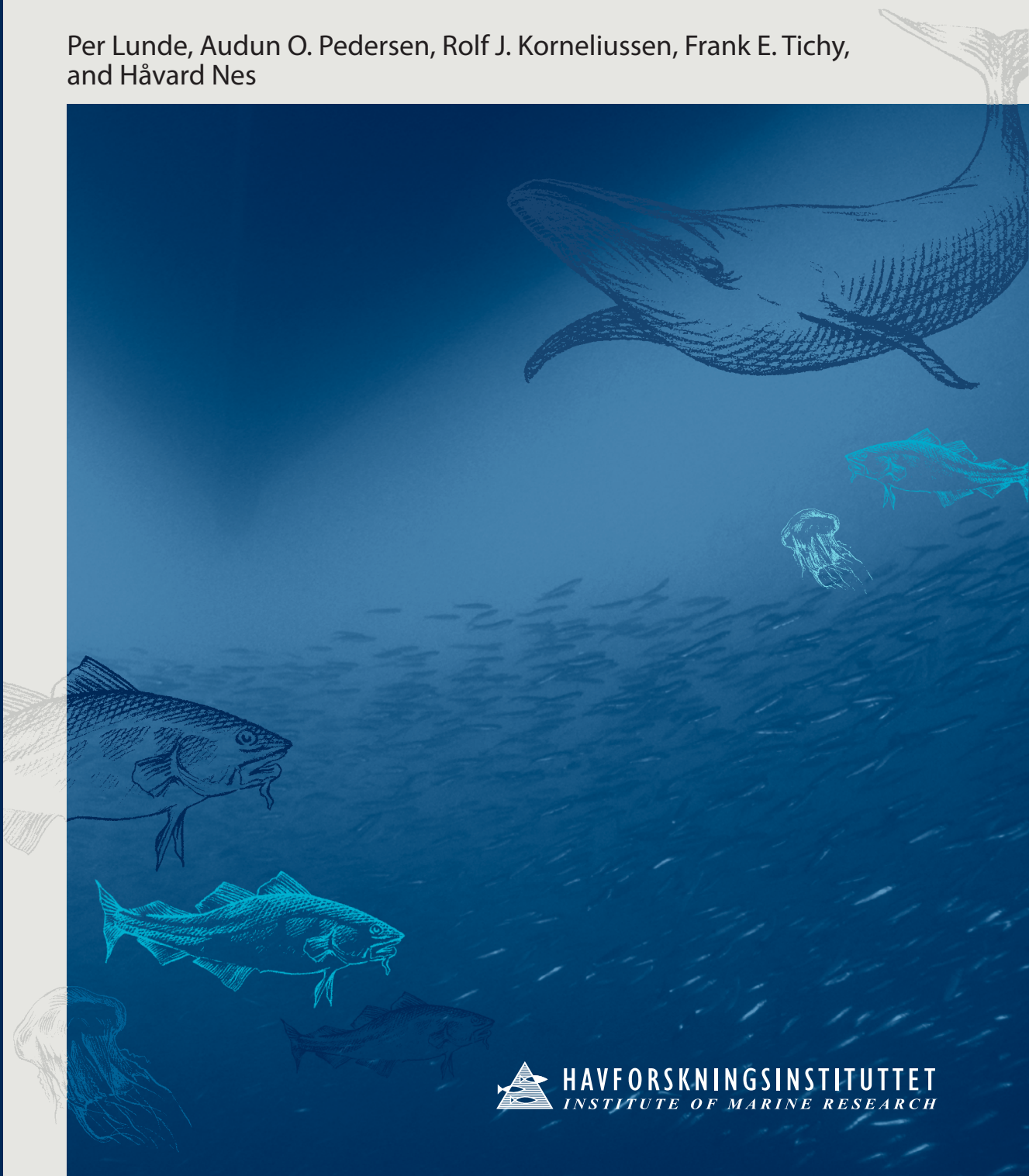


Power-budget and echo-integrator equations for fish abundance estimation

Per Lunde, Audun O. Pedersen, Rolf J. Korneliussen, Frank E. Tichy, and Håvard Nes



This report should be cited as:

P. Lunde, A. O. Pedersen, R. J. Korneliussen, F. E. Tichy, and H. Nes, “Power-budget and echo-integrator equations for fish abundance estimation”, Fisken og Havet no. 10/2013, Institute of Marine Research, Bergen, Norway, 39 p.

http://www.imr.no/publikasjoner/andre_publicasjoner/fisken_og_havet/nb-no



cmr Instrumentation

 **HAVFORSKNINGSINSTITUTTET**
INSTITUTE OF MARINE RESEARCH



Power-budget and echo-integrator equations for fish abundance estimation

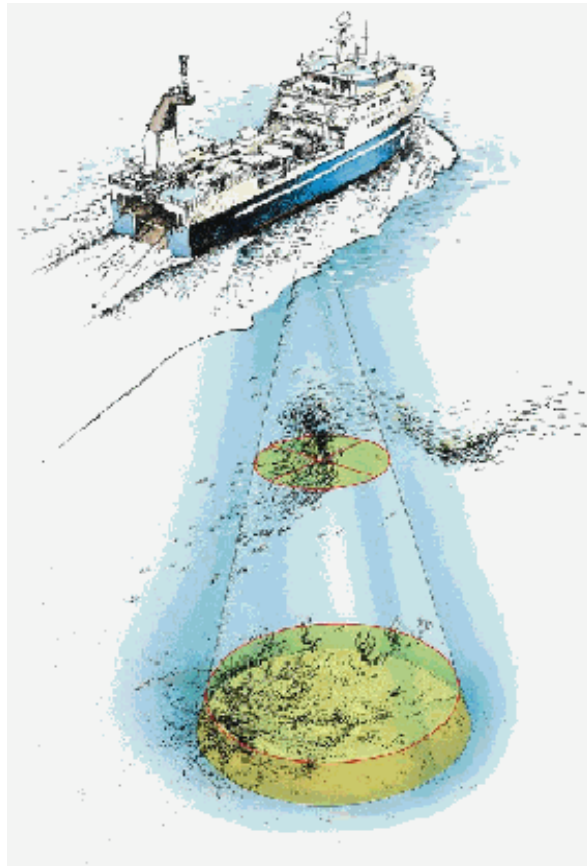
Per Lunde^{1,2,a,b}, Audun O. Pedersen^{2,1,b,c}, Rolf J. Korneliussen³,
Frank E. Tichy⁴, and Håvard Nes⁴

¹ University of Bergen, Dept. of Physics and Technology, P.O.Box 7803, N-5020 Bergen, Norway

² Christian Michelsen Research AS, P.O.Box 6031, Postterminalen, N-5892 Bergen, Norway

³ Institute of Marine Research, P.O.Box 1870, Nordnes, N-5817, Bergen, Norway

⁴ Kongsberg Maritime AS, P.O.Box 111, Strandpromenaden 50, N-3191 Horten, Norway




Ill: Simrad / Kongsberg Maritime AS

a) Corresponding author. Electronic mail: per.lunde@ifit.uib.no

b) Also with *the Michelsen Centre for Industrial Measurement Science and Technology*, Norway.

c) Present address: ClampOn, Vågsgaten 10, N-5160 Laksevåg, Bergen, Norway.

<h1>PROSJEKTRAPPORT</h1>		Distribusjon / Distribution: Åpen / Open												
 <h2>HAVFORSKNINGSINSTITUTTET</h2> <p>INSTITUTE OF MARINE RESEARCH</p> <p>Nordnesgaten 50, Postboks 1870 Nordnes, 5817 BERGEN Tlf. 55 23 85 00, Fax 55 23 85 31, www.imr.no</p> <table style="width: 100%; border: none;"> <tr> <td style="text-align: center;">Tromsø</td> <td style="text-align: center;">Flødevigen</td> <td style="text-align: center;">Austevoll</td> <td style="text-align: center;">Matre</td> </tr> <tr> <td style="text-align: center;">9294 TROMSØ</td> <td style="text-align: center;">4817 HIS</td> <td style="text-align: center;">5392 STOREBØ</td> <td style="text-align: center;">5984 MATREDAL</td> </tr> <tr> <td style="text-align: center;">Tlf. 55 23 85 00</td> <td style="text-align: center;">Tlf. 37 05 90 00</td> <td style="text-align: center;">Tlf. 55 23 85 00</td> <td style="text-align: center;">Tlf. 55 23 85 00</td> </tr> </table>		Tromsø	Flødevigen	Austevoll	Matre	9294 TROMSØ	4817 HIS	5392 STOREBØ	5984 MATREDAL	Tlf. 55 23 85 00	Tlf. 37 05 90 00	Tlf. 55 23 85 00	Tlf. 55 23 85 00	HI-prosjektnummer: N/A
		Tromsø	Flødevigen	Austevoll	Matre									
		9294 TROMSØ	4817 HIS	5392 STOREBØ	5984 MATREDAL									
		Tlf. 55 23 85 00	Tlf. 37 05 90 00	Tlf. 55 23 85 00	Tlf. 55 23 85 00									
Oppdragsgiver(e): N/A														
Oppdragsgivers referanse: N/A														
		Dato / Date: 31.12.2013												
Rapport / Report: Fisken og havet	Nr. 10/2013	Program: N/A												
Title / Tittel: Power-budget and echo-integrator equations for fish abundance estimation Effektbudsjett- og ekkointegrator-ligninger for akustisk bestandsestimering av fisk		Forskningsgruppe / Research group: Marin økosystemakustikk/ Observation methodology												
Per Lunde ^{1,2} , Audun O. Pedersen ^{2,1} , Rolf J. Korneliussen ³ , Frank E. Tichy ⁴ , and Håvard Nes ⁴ ¹ University of Bergen (UoB), Dept. of Physics and Technology, Norway ² Christian Michelsen Research AS (CMR), Bergen, Norway ³ Institute of Marine Research (IMR), Bergen, Norway ⁴ Kongsberg Maritime AS, Horten, Norway		Antall sider totalt / pages: 40												
Sammendrag (norsk): Kontroll med temperatur- og endelig-amplitude-effekter i havet i forbindelse med akustisk bestandsestimering og artsgjenkjennelse under fiskeritokt, krever at kalibreringsfaktoren C i den konvensjonelle ekkointegrator-ligningen for vitenskapelige ekkolodd, er fullt ut kjent og gitt i form av sonarsystemets elektriske og akustiske parametre. Da tilstrekkelige funksjonsuttrykk ikke er kjent eller tilgjengelig fra i tidligere litteratur, re-visiteres her den teoretiske basis for effektbudsjett- og ekkointegrasjons-ligningene som benyttes på dette området. Formålet er (a) å gi en utledning av et mer komplett funksjonsuttrykk for akustisk bestandsestimering, inklusiv uttrykk for kalibreringsfaktoren C ; (b) å ivareta elektrisk terminering; (c) å formulere disse ligningene i form av ekkointegrasjon basert på elektriske spenningssignal; og (d) med dette generalisere Clay og Medwins formulering basert på ekkointegrasjon av lydtrykkssignal i sjøen, til også å ta hensyn til egenskapene til transduseren og de elektroniske komponentene i ekkolodd-systemet. Under antaking om lineære lydforplantningsforhold i sjøen (små lydtrykksamplituder), utledes elektroakustiske effektbudsjett-ligninger for tilbakespredningstverrsnittet i enkelt-objekt tilbakespredning, som brukes under kalibrering av ekkolodd; og volumtilbakespredningskoeffisienten for multippel-objekt tilbakespredning, som brukes for bestandsestimering under tokt. En mer komplett ekkointegrasjons-ligning utledes så fra disse funksjonsuttrykkene, for to operasjonelle tilfeller: "short-ping-and-long-gate", og "long-ping-and-short-gate". Resultatene er konsistente med og generaliserer tidligere arbeid på området.														

Summary (English):

For abundance estimation and species identification on fisheries acoustic surveys, control with temperature and finite amplitude effects in the sea demands the calibration factor C of the conventional echo-integrator equation to be fully known in terms of the sonar system's electrical and acoustical parameters. As no such expression is available from earlier literature, the theoretical basis for the power budget and echo-integrator equations is revisited. The objective is to provide (a) a derivation of these equations for integration in a more complete functional relationship for abundance measurement, including an expression for the calibration factor C ; (b) to account for electrical termination; (c) to formulate these expressions in terms of voltage signal echo integration processing; and (d) thereby generalize the Clay-Medwin formulations based on echo integration of "in-water" sound pressure signals, to account for the transducer and electronics components of the echosounder system. Under conditions of small-amplitude (linear) sound propagation, electroacoustic power budget equations are derived for the backscattering cross section in single-target backscattering, used in echosounder calibration; and the volume backscattering coefficient for multiple-target backscattering, used in oceanic surveys. On this basis a more complete echo-integrator equation is derived for two operational cases, "short-ping-and-long-gate", and "long-ping-and-short-gate". The results are consistent with and extend previous work in this area.

Emneord (norsk):

- Tilbakespredning
- Volumspredning
- Ekkolodd
- Effektbudsjett
- Ekkointegrasjon
- Akustisk deteksjon av marint liv
- Bestandsestimering av fisk

Subject heading (English):

- Backscattering
- Volume scattering
- Echosounder
- Power budget equation
- Echo integrator equation
- Acoustical detection of marine life
- Fish abundance estimation

Per Lunde
Project leader (CMR/UoB)

Espen Johnsen
Research group leader (IMR)

Contents

Abstract.....	7
1 Introduction	8
2 Single-target backscattering	11
2.1 Acoustic backscattering from a single target in the far field.....	12
2.2 Electroacoustic transmit-receive transfer functions for single-target backscattering... 16	
2.3 Electroacoustic power budget equation for single-target backscattering	19
3 Multiple-target (volume) backscattering.....	20
3.1. Electroacoustic power budget equation for volume backscattering.....	21
3.2 Volume backscattering coefficient.....	23
4 Formulation in terms of echo integration	23
4.1 “Short ping and long gate” ($\tau_p \ll \tau_g$).....	24
4.2 “Long ping and short gate” ($\tau_p \gg \tau_g$).....	25
5 Implications for the echo-integrator equation	26
6 Discussion.....	27
6.1 Consistency with previous work.....	27
6.2 Electrical impedance factors, F_{II} and F_{VV}^2	29
6.3 Transducer gain, $G(\theta, \varphi)$	31
6.4 Assumptions underlying the analysis.....	32
7 Conclusions	33
APPENDIX A. Sonar equation for single-target backscattering	37
APPENDIX B. Comparison with the Clay-Medwin acoustic power budget equations	38

Abstract

For abundance estimation and species identification on fisheries acoustic surveys, control with temperature and finite amplitude effects in the sea demands the calibration factor C of the conventional echo-integrator equation to be fully known in terms of the sonar system's electrical and acoustical parameters. As no such expression is available from earlier literature, the theoretical basis for the power budget and echo-integrator equations is revisited. The objective is to provide (a) a derivation of these equations for integration in a more complete functional relationship for abundance measurement, including an expression for the calibration factor C ; (b) to account for electrical termination; (c) to formulate these expressions in terms of voltage signal echo integration processing; and (d) thereby generalize the Clay-Medwin formulations based on echo integration of "in-water" sound pressure signals, to account for the transducer and electronics components of the echosounder system. Under conditions of small-amplitude (linear) sound propagation, electroacoustic power budget equations are derived for the backscattering cross section in single-target backscattering, used in echosounder calibration; and the volume backscattering coefficient for multiple-target backscattering, used in oceanic surveys. On this basis a more complete echo-integrator equation is derived for two operational cases, "short-ping-and-long-gate", and "long-ping-and-short-gate". The results are consistent with and extend previous work in this area.

1 Introduction

Acoustic methods are widely used for estimating fish abundance [1-7], and constitute a key part of the analytic assessment that makes the basis for international regulations of marine resources. For fish aggregated in schools or layers, echo integration [6,7] supported by biological sampling, is the normal method used in oceanic surveys [2]. The acoustic methods rely on calibrated systems [8,9]. Once the acoustic data are interpreted and the scatterers identified, the resulting acoustic values are used for estimating fish stock abundance. This is normally done using the echo-integrator equation [7,9,2,10],

$$\rho_a = \frac{C \bar{g}}{\psi \langle \sigma_{bs} \rangle} E, \quad (1)$$

valid for scattering objects in the far field of the echosounder. Here, ρ_a is the density of targets expressed as the number of fish specimen per unit area over the depth channel being sampled, C is a calibration factor which depends on the sonar parameters (transducer properties, electronic components, sea water properties, frequency, pulse duration, echo integration duration, electrical operating power level, etc.), \bar{g} is the time-varied gain (TVG) correction factor, ψ is the two-way equivalent solid beam angle of the transducer, and $\langle \sigma_{bs} \rangle$ is the expected value of the backscattering cross section of individual fish. E is the echo-integrator output, i.e., the echo-integral of the squared amplitude of the received electrical voltage signal $V_R(t)$ with respect to time, $\int_{t_{g1}}^{t_{g2}} |V_R(t)|^2 dt$, including TVG, averaged over many transmissions. The time gate t_{g1} to t_{g2} is chosen to correspond to the depth channel to be sampled. The measurements of C , \bar{g} and ψ come from the equipment calibration [10].

While use of a calibration factor C in Eq. (1) may be sufficient for many applications [7,9,10], there are situations where documentation of a more complete functional relationship for the abundance measurement is required, such as for investigation of and correction for measurement errors due to finite amplitude (nonlinear) sound propagation effects [11]. These errors may become important at higher frequencies (typically above 100 kHz) and electrical transmission power levels of a few hundred watts and higher [11-16].

One might argue that since scientific echosounders used for fisheries abundance estimation and species identification are being calibrated [9], a functional relationship for C is not needed. However, this works only as long as the echosounder is operated in the linear range, i.e., for small-amplitude waves. To know whether this is the case or not for a given electrical transmit power, a documented functional relationship for C in terms of echosounder parameters is required. Moreover, in cases where the echosounder is actually operated under finite amplitude conditions, either during calibration or in oceanic surveys or both, a documented functional relationship for C under such conditions is needed, to enable correction for measurement errors caused by the finite amplitude effects.

In other situations, effects of water temperature may become significant for the echosounder system performance, and compensation for the temperature dependence of the system may be warranted. Appreciable shifts in echosounder system gains may result from shifts in the transducer frequency response with sea temperature [17], in particular for narrowband transducers, as generally used in fisheries acoustics, operated close to the transducer's resonance frequency. The transducer's beam pattern may also change with temperature changes. As pointed out by Demer and Renfree [17]; since it is standard practice to calibrate echosounder systems for fishery surveys in one environment (typically a sheltered area), and apply the resulting gains to interpret data collected over the range of sea temperatures encountered during a survey, the resulting fish abundance estimates may be biased.

The situations indicated above, are all examples of conditions where a calibration value for C only, is not sufficient. In such cases C needs to be fully known in terms of the echosounder system parameters, i.e., the properties of the transducer, electronics, sea water, electrical signal, echo integration method, acoustic sound field, etc. That is, mathematically, in terms of a functional relationship. As no functional relationship for C has been given in earlier literature, derivation of such a relationship for small-amplitude sound waves is addressed here.

The basic acoustic measurand in abundance estimation is the volume backscattering coefficient, s_v , which in current scientific echosounders is calculated from time integration of the transmitted and received electrical voltage signals measured at the transducer terminals (echo integration), by means of an expression referred to as the power budget equation for volume backscattering [18,19,11,10,20]. For on-ship calibration of scientific echosounders prior to oceanic surveys using standard targets (solid spheres), a corresponding power budget equation for single-target backscattering is used [20,17].

These power budget equations for single-target and volume backscattering can be used to determine C in terms of the echosounder parameters, given that the equations account for all parameters of importance, and that sufficient documentation of these equations is provided. A textbook or journal publication with derivation or documentation of such expressions, for conditions of electroacoustic wave propagation, does however not seem to be available.

Derivation of expressions for s_v which account for the sound propagation in the fluid medium only (sea water), in terms of acoustic pressures, has been given by Clay and Medwin [21,22]. The electrical and transducer parts of the electroacoustic echosounder system were not considered, such as the transmitting and receiving responses of the transducer, the measured transmit and receive electrical powers, and transducer and electrical termination impedances. These "in-water" expressions, which are not sufficient for determination of the calibration coefficient C in Eq. (1), will here be referred to as the "acoustic power budget equations" for volume backscattering.

A derivation of an expression for s_v which, in addition to the sound propagation in the fluid medium, accounts for electronics and transducer parts of the echosounder system, such as the transducer's transmit and receive responses, and the measured transmit and receive electrical powers, was given by Simrad [18] in their EK 500 scientific echosounder instruction manual. The approach was based on the radar equation used in electromagnetic theory, *ad hoc* adapted to acoustic conditions. The electrical impedances of the transducer and the receiving electronics were not accounted for, so the expression is valid under certain conditions of electrical termination. Time integration of the transmit and receive voltage signals (echo integration) was not described. A summary of the Simrad derivation was given by Korneliussen [19]. The same expression was used by Simmonds and MacLennan [10] and Ona *et al.* [20], however without a derivation or a reference to its origin. A similar, but different, expression was used by Demer and Renfree [17].

An extended expression for s_v was derived by Pedersen [11] from acoustic principles, where also the electrical impedances of the transducer and the receiving electronics were accounted for, however with some minor irregularities in the derivation. Echo integration of the transmit and receive voltage signals was not accounted for.

To distinguish the above expressions from the “in-water” expressions given by Clay and Medwin [21,22] for the acoustic pressure, the expressions derived in [18,11] and similar will here be referred to as “electroacoustic power budget equations” for volume backscattering.

The derivations of the electroacoustic power budget equations [18,11] are based on a frequency domain description using continuous waves, applicable also to the steady-state portions of finite-duration signals. The “in-water” acoustic power budget equations given by Clay and Medwin [21,22] are time domain descriptions, based on “time-integral-pressure-squared” [*tips*] “processing” (sound pressure echo integration). In practice, echo integration is based on the squared *voltage* signals [10], which, - in analogy with the Medwin and Clay terminology [22], will here be referred to as “time-integral-voltage-squared” [*tivs*] processing (voltage echo integration).

The objectives of the present work are

- (1) to provide a consistent and relatively complete derivation of the electroacoustic power budget equations for single-target and volume backscattering routinely used in echosounder calibration and oceanic surveys, for integration in a more complete functional relationship for abundance measurements, where the calibration factor C of the conventional echo-integrator equation is specified fully in terms of the echosounder's electrical and acoustical parameters,
- (2) to extend previous theory [18,11] to account for more general conditions of electrical termination, and echo integration,

- (3) to express these electroacoustic power budget equations for single-target and volume backscattering, in terms of voltage signal echo integration [*tivs*] instead of electrical powers, and thereby
- (4) generalize the “in-water” acoustic power budget equations derived by Clay and Medwin [21,22], based on time integration of sound pressure signals, [*tips*], to electroacoustic power budget equations based on the more relevant voltage signal echo integration [*tivs*] approaches used in scientific echosounder systems, and
- (5) in terms of relatively complete functional relationships for fish abundance measurement, give a theoretical fundament for investigation of errors due to (a) finite amplitude effects in fisheries research, and (b) possible sea temperature deviations between calibration and survey operation situations, and thereby provide a basis for investigating and compensating for such possible errors in fisheries research.

A frequency domain approach is used to enable utilization of existing theory for reciprocal transducers, transducer responses, electrical circuits, etc., in the description of the sonar. The intention is to present a derivation from fundamental acoustic principles, for signal propagation in the echosounder and the fluid medium, to clearly reveal the assumptions and approximations on which the derivation relies. These may not have been fully stated in previous work related to the electroacoustic power budget equations. The analysis includes investigation of under which conditions of electrical termination the expressions derived by Simrad [18] (and used by e.g. Korneliussen [19], Simmonds and MacLennan [10], Ona *et al.* [20], Demer and Renfree [17]) are valid. The expressions are then further developed to account for more general conditions of electrical termination than in [11], and echo integration based on [*tivs*] processing. Two cases of [*tivs*] echo integration are considered: “short ping and long gate”, and “long ping and short gate” [21].

The outline of the report is the following: derivation of the electroacoustic power budget equation for backscattering from a single target (Section 2); use of this expression to derive the electroacoustic power budget equation for volume backscattering from a multitude of targets, in terms of frequency-domain (Section 3) and time-domain (Section 4) descriptions; use of these results in the echo-integrator equation (Section 5); discussion of the results in relation to previous literature, interpretation of quantities involved, and assumptions underlying the theory (Section 6); and conclusions of the work (Section 7). Two appendices A and B are included for interpretation and discussion of the results.

2 Single-target backscattering

A frequency domain description is used, with time harmonic factor $e^{i\omega t}$, where $i = \sqrt{-1}$, $\omega = 2\pi f$ is the angular frequency, f is the frequency, and t is the time. Bold-face letters are used to indicate complex-valued quantities, and vectors are represented by underlined

characters. Small-amplitude sound pressure waves are assumed, so that the linearized theory of sound propagation applies, and finite amplitude effects can be neglected.

2.1 Acoustic backscattering from a single target in the far field

Consider the situation shown in Figure 1. An electric signal at angular frequency ω is fed to an electroacoustic transducer, by which it is converted to an acoustic pressure wave, and radiated into a homogeneous fluid medium (i.e., with constant density and sound velocity). In the fluid, at arbitrary position in the far field of the transducer (on or off axis), consider a single object of unspecified shape and material, or alternatively, a multitude of such objects of different types, materials and sizes, confined to a sufficiently small volume in space, so that the sound backscattered from the object(s) to the transducer appears as if the scattering came from a single target [23]. This object, or small volume of objects, can then be treated as a single target, and will for convenience be referred to as “the target”. In the far field of the target, the scattered pressure field will spread spherically. The backscattered sound pressure wave is received by the same transducer, and converted to an electric signal.

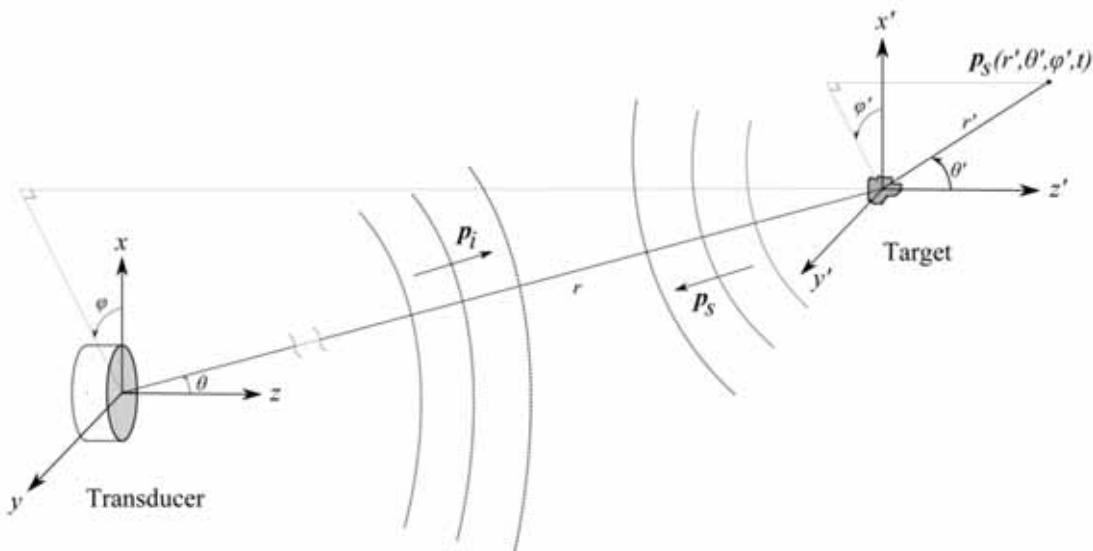


Figure 1. Sketch of the acoustic system for single-target backscattering, with an electroacoustic transducer operating as transmitter and receiver of ultrasound, acoustic backscattering from a single scattering object (target) in a homogeneous fluid medium, and the two spherical coordinate systems 1 and 2 used for the transmitted and scattered sound wave fields, respectively. The target centre is located at position (r, θ, φ) relative to coordinate system no. 1.

Two coordinate systems are used to describe this electroacoustic system. The origin of coordinate system no. 1, used for the transmitted wave field, is located at the center of the front face of the transducer. The z-axis is taken along the transducer’s acoustic beam axis. Coordinate system no. 2, used for the scattered wave field, and employing primed coordinates, is parallel to coordinated system no. 1, and with origin located at the centre of the target. The figure shows the Cartesian coordinates x , y , and z (x' , y' , and z') and the spherical coordinates r , θ and φ (r' , θ' and φ') for the two coordinate systems, where r (r') is the radial distance, denoted range, θ (θ') is the polar angle, and φ (φ') is the azimuthal angle. The

position vectors in the two coordinate systems are $\underline{r}=(r,\theta,\varphi)$ and $\underline{r}'=(r',\theta',\varphi')$, respectively, with $x=r\sin\theta\cos\varphi$, $y=r\sin\theta\sin\varphi$, $z=r\cos\theta$, $\theta\in[0,\pi]$, $\varphi\in[0,2\pi]$, and $x'=r'\sin\theta'\cos\varphi'$, $y'=r'\sin\theta'\sin\varphi'$, $z'=r'\cos\theta'$, $\theta'\in[0,\pi]$, $\varphi'\in[0,2\pi]$.

Under these assumptions, using subscripts “*i*” and “*s*” for incident and scattered waves, respectively, the incident pressure wave, \mathbf{p}_i , and the scattered pressure wave, \mathbf{p}_s , are given as

$$\mathbf{p}_i(r,\theta,\varphi,t)=\mathbf{P}_i(r,\theta,\varphi)\cdot e^{i(\omega t-\underline{k}\cdot\underline{r})}, \quad \mathbf{P}_i(r,\theta,\varphi)=\frac{A_i}{r}\cdot e^{-\alpha r}\cdot \mathbf{B}_i(\theta,\varphi), \quad (2)$$

$$\mathbf{p}_s(r',\theta',\varphi',t)=\mathbf{P}_s(r',\theta',\varphi')\cdot e^{i(\omega t-\underline{k}\cdot\underline{r}')}, \quad \mathbf{P}_s(r',\theta',\varphi')=\frac{A_s(r)}{r'}\cdot e^{-\alpha r'}\cdot \mathbf{B}_s(\theta',\varphi'), \quad (3)$$

respectively, where \mathbf{P}_i and \mathbf{P}_s are the sound pressure amplitudes, A_i is a complex constant, $A_s(r)$ is a complex function of range, r , which for increasing r decreases in magnitude proportional to $\mathbf{P}_i(r,\theta,\varphi)$, and

$$\mathbf{B}_i(\theta,\varphi)\equiv\frac{\mathbf{P}_i(r,\theta,\varphi)}{\mathbf{P}_i(r,0,0)}, \quad \mathbf{B}_s(\theta',\varphi')\equiv\frac{\mathbf{P}_s(r',\theta',\varphi')}{\mathbf{P}_s(r',0,0)} \quad (4)$$

are the beam patterns of the incident and scattered sound pressure waves, respectively. $\mathbf{P}_i(r,0,0)$ is the axial sound pressure amplitude for the incident sound field. $\mathbf{P}_s(r',0,0)$ is the sound pressure amplitude along the z' axis, for the scattered sound field. $\underline{k}=k\underline{e}_k$ is the acoustic wave number vector, where \underline{e}_k is the unit vector normal to the wavefront, $k=|\underline{k}|=\omega/c_0$ is the acoustic wave number, c_0 is the small-amplitude sound velocity of the fluid, and α is the acoustic absorption coefficient of the fluid (expressed in Np/m) [24].

The use of $\mathbf{P}_s(r',0,0)$ as normalization pressure amplitude in the second of Eqs. (4) may need a comment, since the z' axis is not necessarily the direction of maximum scattering. This approach has been chosen for convenience and without loss of generality, since the results derived in the following become independent of the choice of normalization direction for $\mathbf{B}_s(\theta',\varphi')$.

In general, \mathbf{P}_i , \mathbf{P}_s , A_i , A_s , \mathbf{B}_i , \mathbf{B}_s and α , are all functions of the angular frequency ω , but for convenience in notation, this ω -dependency is omitted in the equations.

The intensity of the incident wave at a target located in the transducer’s far field, with center at position (r,θ,φ) relative to coordinate system no. 1, and the intensity of the scattered wave in the target’s far field, at position (r',θ',φ') relative to coordinate system no. 2, are

$$I_i = \frac{|\mathbf{P}_i(r, \theta, \varphi)|^2}{2\rho_0 c_0}, \quad I_s = \frac{|\mathbf{P}_s(r', \theta', \varphi')|^2}{2\rho_0 c_0} = \frac{|\mathbf{A}_s(r)|^2}{2\rho_0 c_0} \cdot \frac{e^{-2\alpha r'}}{r'^2} \cdot |\mathbf{B}_s(\theta', \varphi')|^2, \quad (5)$$

respectively, where ρ_0 is the ambient density of the fluid. From Eqs. (5), the intensity of the scattered field extrapolated spherically back to a reference range r_0' (e.g. 1 m) from the target, $I_{s,0} \equiv I_s(r_0', \theta', \varphi')$, is given as

$$I_{s,0} = I_i \cdot \frac{e^{-2\alpha r_0'}}{r_0'^2} \cdot S_s(\theta, \varphi, \theta', \varphi', \omega) \cdot A, \quad S_s \cdot A \equiv \left| \frac{\mathbf{A}_s(r) \cdot \mathbf{B}_s(\theta', \varphi')}{\mathbf{P}_i(r, \theta, \varphi)} \right|^2 \quad (6)$$

where S_s is the scattering function, and A is the cross section area of the scattering target, viewed from the transducer. Note that S_s is independent of range, r , since the ratio $|\mathbf{A}_s(r)/\mathbf{P}_i(r, \theta, \varphi)|$ is independent of r .

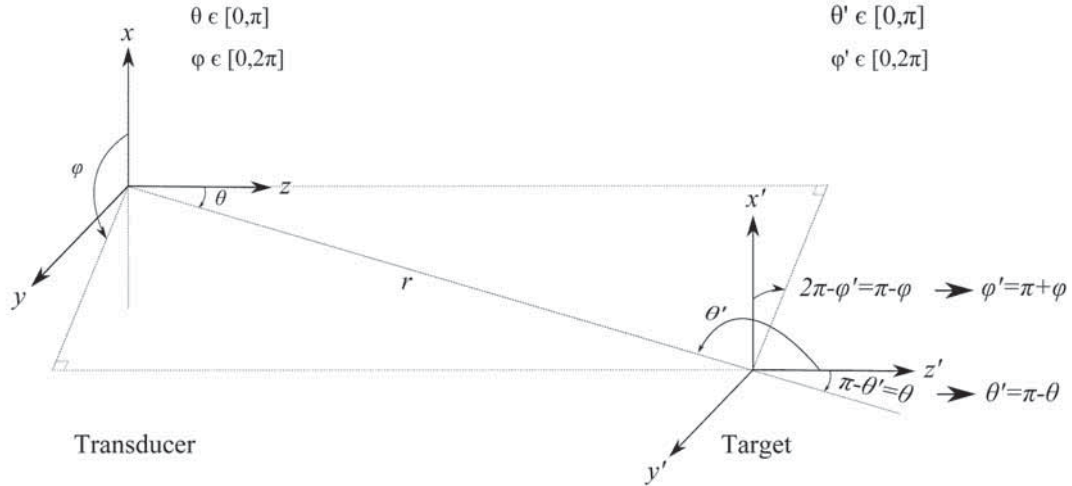


Figure 2. Sketch of arbitrary transducer - target positions, giving the relationship between (θ, φ) and (θ', φ') for backscattering from a single target at arbitrary location (r, θ, φ) . From the figure, the backscattering direction is given as $\theta' = \pi - \theta$, $\varphi' = \pi + \varphi$.

From Figure 2, the backscattering direction is given by $\theta' = \pi - \theta$ and $\varphi' = \pi + \varphi$. The back-scattered intensity $I_{bs,0} \equiv I_s(r_0', \theta' = \pi - \theta, \varphi' = \pi + \varphi)$ at the reference range r_0' from the target is given as

$$I_{bs,0} = I_i \cdot \frac{e^{-2\alpha r_0'}}{r_0'^2} \cdot \sigma_{bs}, \quad (7)$$

where

$$\sigma_{bs} \equiv S_{bs} \cdot A = \frac{I_{bs,0}}{I_i} \cdot r_0'^2 \cdot e^{2\alpha r_0'}, \quad S_{bs} \equiv S_s(\theta, \varphi, \theta' = \pi - \theta, \varphi' = \pi + \varphi, \omega), \quad (8)$$

are the backscattering cross section of the target and the backscattering function, respectively. σ_{bs} depends in general on frequency, the direction (θ, φ) of the incident wave, and the shape of the target.

Note that in this description, absorption and spherical spreading of the scattered field are omitted from σ_{bs} , so that σ_{bs} does not include these effects. Absorption and spherical spreading in backscattering are accounted for in $I_{bs,0}$, as seen from Eq. (7).

By use of Eqs. (5) in Eq. (8), σ_{bs} can be expressed in terms of pressure amplitudes instead of intensities, giving

$$|\mathbf{P}_{bs,0}| = |\mathbf{P}_i| \cdot \frac{e^{-\alpha r_0'}}{r_0'} \cdot \sqrt{\sigma_{bs}}, \quad (9)$$

where $\mathbf{P}_{bs,0}$ is the backscattered sound pressure amplitude at the reference range r_0' from the target. From Eq. (2), the incident pressure amplitude at the target can be written as

$$\mathbf{P}_i = \mathbf{P}_{i,0} \cdot \frac{r_0}{r} \cdot e^{-\alpha(r-r_0)} \cdot \mathbf{B}_i(\theta, \varphi), \quad (10)$$

where

$$\mathbf{P}_{i,0} \equiv \mathbf{P}_i(r_0, 0, 0) = \frac{\mathbf{A}_i}{r_0} \cdot e^{-\alpha r_0} \quad (11)$$

is the axial sound pressure amplitude transmitted by the transducer at the reference range r_0 (e.g. 1 m) from the transducer front, extrapolated spherically from the far field.

Similarly, from Eq. (3), the backscattered pressure amplitude at a range r' relative to coordinate system no. 2 can be written as

$$\mathbf{P}_{bs} = \mathbf{P}_{bs,0} \cdot \frac{r_0'}{r'} \cdot e^{-\alpha(r'-r_0')}. \quad (12)$$

By insertion of Eqs. (10) and (12) in Eq. (9), and setting r' equal to r , the magnitude of the amplitude of the backscattered free-field sound pressure in the fluid at the center of the transducer front (i.e., in absence of the transducer), $\mathbf{P}_{bs} = \mathbf{P}_{bs}(0, 0, 0)$, becomes

$$|\mathbf{P}_{bs}| = |\mathbf{P}_{i,0}| \cdot |\mathbf{B}_i(\theta, \varphi)| \cdot \frac{r_0}{r^2} \cdot e^{-\alpha(2r-r_0)} \cdot \sqrt{\sigma_{bs}}. \quad (13)$$

Equation (13) gives the sound pressure amplitude backscattered from a single target located in the far field, under small-amplitude (linear) sound propagation conditions. For reference, it is noted that Eq. (13) can equivalently be written on a logarithmic (dB) sonar equation form, cf. Appendix A.

2.2 Electroacoustic transmit-receive transfer functions for single-target backscattering

In the following, Eq. (13) is used to develop electroacoustic transmit-receive transfer functions for backscattering from a single target in the far field, by accounting for (a) the transmitting and receiving responses of the transducer, (b) the beam pattern upon reception, (e) the transducer efficiency, (f) spherical reciprocity, (c) the transmit electrical power, and (d) the electrical impedances of the transducer and the receiving electronics.

Assume the transducer is linear, passive and reversible, and fulfills the reciprocity relationships [25]. The transducer's axial transmitting current response, S_I , and open-circuit free-field receiving voltage sensitivity, M_V , are given as [25]

$$S_I = \frac{P_{i,0}}{I_T}, \quad M_V = \frac{V_0}{P_{bs}} = M_V^{ax} \cdot B_i(\theta, \varphi), \quad (14)$$

respectively, where I_T is the input current to the transducer during transmission, V_0 is the received voltage across the transducer terminals under open-circuit conditions, and M_V^{ax} is the open-circuit free-field receiving voltage sensitivity for pressure waves incident along the acoustic axis (normally incident waves, $\theta=0, \varphi=0$). $B_i(\theta, \varphi)$ is the beam pattern of the transducer upon reception, which is equal to the beam pattern upon transmission [25] and thus given by the first of Eqs. (4). Insertion of Eqs. (14) into (13) leads to the open-circuit transmit-receive transfer function

$$\left| \frac{V_0}{I_T} \right| = |M_V^{ax}| \cdot |S_I| \cdot |B(\theta, \varphi)|^2 \cdot \frac{r_0}{r^2} \cdot e^{-\alpha(2r-r_0)} \cdot \sqrt{\sigma_{bs}}. \quad (15)$$

The transducer's electroacoustic efficiency under lossless conditions in the fluid is defined as

$$\eta = \frac{\Pi_a}{\Pi_T}, \quad (16)$$

where [26]

$$\Pi_T = \frac{|V_T|^2 R_T}{2|Z_T|^2} = \frac{1}{2} R_T |I_T|^2 \quad (17)$$

is the electrical power delivered to the transducer during transmission (here denoted “transmit electrical power”), V_T and I_T are the electrical voltage and current amplitudes at the electrical terminals of the transmitting transducer, and R_T is the real part (resistance) of the transducer’s input electrical impedance when radiating into the fluid, $Z_T \equiv V_T/I_T = R_T + iX_T$, cf. Figure 3a. Π_a is the total acoustic power radiated from the transducer under assumed lossless conditions in the fluid, given in the far field as [26]

$$\Pi_a = \int_{4\pi} \frac{|P_i(r, \theta, \varphi)|^2 e^{2\alpha r}}{2\rho_0 c_0} r^2 d\Omega, \quad (18)$$

where $d\Omega = \sin\theta d\theta d\varphi$ is a small element of the solid angle Ω . From Eqs. (2), (16) and (18) one obtains

$$\eta = \frac{2\pi r^2 |P_i(r, 0, 0)|^2 e^{2\alpha r}}{\rho_0 c_0 \cdot \Pi_T \cdot D}, \quad (19)$$

where the directivity factor D of the transmitted field is defined as [26]

$$D \equiv \frac{4\pi}{\int_{4\pi} |B_i(\theta, \varphi)|^2 d\Omega}. \quad (20)$$

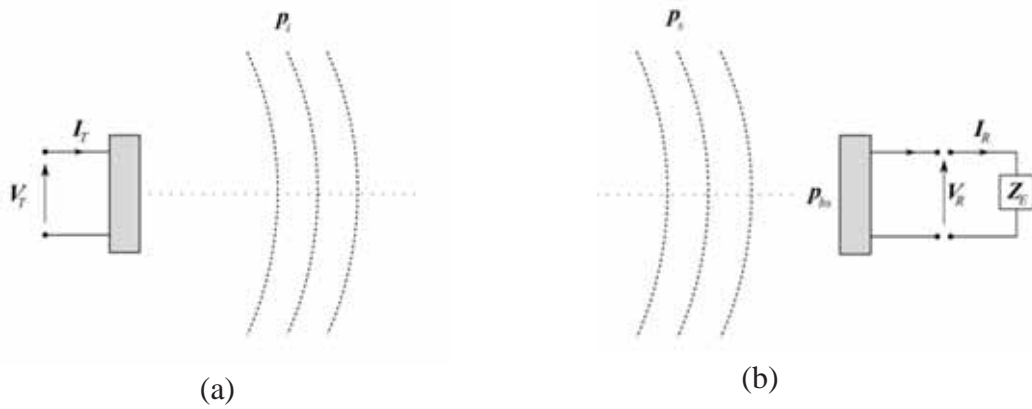


Figure 3. Sketch of the electrical connections for the electroacoustic transducer operating in (a) transmit and (b) receive modes.

Combining the first of Eqs. (14) with Eqs. (17) and (19) leads to

$$|S_I|^2 = \frac{\eta \cdot D \cdot R_T \cdot \rho_0 c_0 \cdot e^{-2\alpha r_0}}{4\pi r_0^2}. \quad (21)$$

Since $P_{i,0}$ on which S_I is based (cf. Eq. (14)) is extrapolated from the far field, the spherical-wave reciprocity relationship applies, stating that [25,27,28]

$$\frac{\mathbf{M}_V^{ax}}{\mathbf{S}_I} = \mathbf{J}_s \equiv \frac{2r_0\lambda}{i\rho_0c_0} e^{ikr_0} e^{c\alpha r_0}, \quad (22)$$

where \mathbf{J}_s is the spherical-wave reciprocity parameter, and $\lambda = c_0/f$ is the acoustic wavelength. By insertion of Eqs. (21) and (22) into Eq. (15) the open-circuit transmit-receive transfer function becomes

$$\left| \frac{\mathbf{V}_0}{\mathbf{I}_T} \right| = 2R_T \cdot G(\theta, \varphi) \cdot \frac{\lambda}{4\pi} \cdot \frac{e^{-2c\alpha r}}{r^2} \cdot \sqrt{\sigma_{bs}}, \quad (23)$$

where the transducer gain [29], $G(\theta, \varphi)$, is defined as

$$G(\theta, \varphi) \equiv \eta \cdot \frac{4\pi |\mathbf{B}_i(\theta, \varphi)|^2}{\int_{4\pi} |\mathbf{B}_i(\theta, \varphi)|^2 d\Omega} = \eta \cdot D \cdot |\mathbf{B}_i(\theta, \varphi)|^2. \quad (24)$$

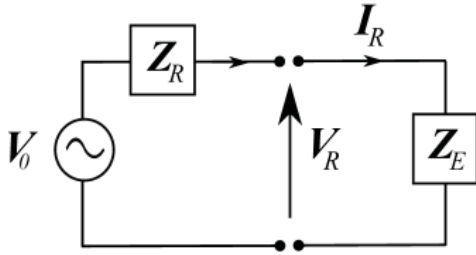


Figure 4. Helmholtz-Thevenin equivalent model for the electroacoustic transducer upon signal reception.

To include effects of non-ideal electrical termination at the receiver, consider the situation indicated in Figure 3b, which can be represented electrically by the Helmholtz-Thevenin equivalent circuit shown in Figure 4. Here, $\mathbf{Z}_R = R_R + iX_R$ is the output electrical impedance of the receiving transducer, R_E is the real part (resistance) of the input electrical impedance of the receiving electrical network, $\mathbf{Z}_E \equiv \mathbf{V}_R / \mathbf{I}_R = R_E + iX_E$, cf. Figure 3b, where \mathbf{V}_R and \mathbf{I}_R are the electrical voltage and current amplitudes at the transducer terminals during reception. From Figure 4, \mathbf{V}_R is given by

$$\frac{\mathbf{V}_R}{\mathbf{V}_0} = \frac{\mathbf{Z}_E}{\mathbf{Z}_R + \mathbf{Z}_E}. \quad (25)$$

Insertion of Eq. (25) and these electrical impedance definitions into Eq. (23) yields

$$\left| \frac{\mathbf{V}_R}{\mathbf{V}_T} \right| = F_{\text{W}} \cdot G(\theta, \varphi) \cdot \frac{\lambda}{4\pi} \cdot \frac{e^{-2c\alpha r}}{r^2} \cdot \sqrt{\sigma_{bs}}, \quad \left| \frac{\mathbf{I}_R}{\mathbf{I}_T} \right| = F_{\text{II}} \cdot G(\theta, \varphi) \cdot \frac{\lambda}{4\pi} \cdot \frac{e^{-2c\alpha r}}{r^2} \cdot \sqrt{\sigma_{bs}} \quad (26a)$$

$$\left| \frac{\mathbf{V}_R}{\mathbf{I}_T} \right| = F_{IV} \cdot G(\theta, \varphi) \cdot \frac{\lambda}{4\pi} \cdot \frac{e^{-2\alpha r}}{r^2} \cdot \sqrt{\sigma_{bs}}, \quad \left| \frac{\mathbf{I}_R}{\mathbf{V}_T} \right| = F_{VI} \cdot G(\theta, \varphi) \cdot \frac{\lambda}{4\pi} \cdot \frac{e^{-2\alpha r}}{r^2} \cdot \sqrt{\sigma_{bs}} \quad (26b)$$

for the magnitudes of the four transmit-receive transfer functions of interest, where

$$F_{VV} \equiv \frac{2R_T |\mathbf{Z}_E|}{|\mathbf{Z}_R + \mathbf{Z}_E| |\mathbf{Z}_T|}, \quad F_{II} \equiv \frac{2R_T}{|\mathbf{Z}_R + \mathbf{Z}_E|}, \quad (27a)$$

$$F_{IV} \equiv \frac{2R_T |\mathbf{Z}_E|}{|\mathbf{Z}_R + \mathbf{Z}_E|}, \quad F_{VI} \equiv \frac{2R_T}{|\mathbf{Z}_R + \mathbf{Z}_E| |\mathbf{Z}_T|} \quad (27b)$$

are defined as electrical impedance factors for the respective transfer functions in Eqs. (26).

The electrical impedance factors represent the influence of finite electrical impedances at transmission and reception. The transducer gain $G(\theta, \varphi)$ represents the transducer's two-way electroacoustic "efficiency" in the (θ, φ) direction, cf. Section 6.3. The term $e^{-2\alpha r}/r^2$ represents two-way amplitude loss due to absorption and spherical spreading, and $\sqrt{\sigma_{bs}}$ represents the target strength in the backscattering direction, cf. Appendix A. λ was introduced through the spherical reciprocity relationship, Eq. (22), and accounts for the proportionality of $P_{i,0}$ with frequency, f . The factor 4π balances the factor 4π in $G(\theta, \varphi)$, cf. Eq. (24).

2.3 Electroacoustic power budget equation for single-target backscattering

By also accounting for the electrical power delivered to the electronics termination load during reception (here denoted "received electrical power"), given as [26]

$$\Pi_R = \frac{|\mathbf{V}_R|^2 R_E}{2|\mathbf{Z}_E|^2}, \quad (28)$$

the transfer functions given by Eqs. (26) can be used to develop an electroacoustic power budget equation. Insertion of Eqs. (17) and (28) into the first of Eqs. (26a) yields the transmit-receive electrical power transfer function

$$\frac{\Pi_R}{\Pi_T} = F_{\Pi} \cdot G^2(\theta, \varphi) \cdot \frac{\lambda^2}{(4\pi)^2} \cdot \frac{e^{-4\alpha r}}{r^4} \cdot \sigma_{bs}, \quad (29)$$

where the electrical impedance factor for the power transfer function is defined as [11]

$$F_{\Pi} \equiv \frac{4R_T R_E}{|\mathbf{Z}_R + \mathbf{Z}_E|^2} . \quad (30)$$

From Eq. (29) the backscattering cross section becomes

$$\sigma_{bs} = \frac{16\pi^2 \cdot r^4 \cdot e^{4\alpha r} \cdot \Pi_R}{G^2(\theta, \varphi) \cdot \lambda^2 \cdot F_{\Pi} \cdot \Pi_T} . \quad (31)$$

Equation (29), or equivalently, Eq. (31), is the electroacoustic power budget equation for backscattering from a single target arbitrarily located in the far field, under conditions of small-amplitude (linear) sound propagation. As explained above, it also covers backscattering from a multitude of objects in the far field confined to a sufficiently small volume in space, so that the backscattering at the transducer appears as if the scattering came from a single target.

3 Multiple-target (volume) backscattering

Now, consider backscattering from a spherical shell volume in the far field, V_{obs} (denoted “observation volume”), between ranges r_{min} and r_{max} (cf. Figure 5), containing a distribution of scattering objects of different types (e.g., different types of fish, krill, zooplankton, etc.). In the present section, Eq. (31) is used to derive an expression for the volume backscattering coefficient for a spherical shell subvolume, V_p , in V_{obs} .

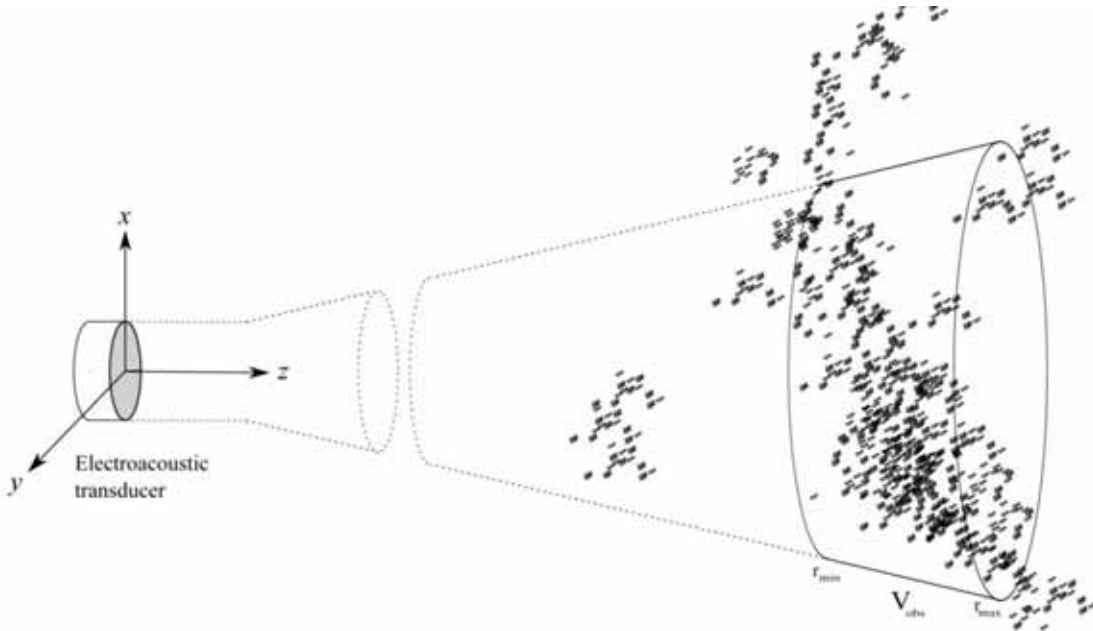


Figure 5. Sketch of the acoustic system under analysis, with an electroacoustic transducer operating as transmitter and receiver of ultrasound, and acoustic volume backscattering from a multitude of scattering objects in a spherical shell observation volume, V_{obs} , which is weighted in (θ, φ) direction by the transducer’s transmit and receive beam patterns.

3.1 Electroacoustic power budget equation for volume backscattering

Assume that (a) the scattered echoes from different objects in V_{obs} have random phases, (b) multiple scattering effects and interaction between objects can be neglected, and (c) excess attenuation from power extinction [21] caused by volume scattering in V_{obs} can be neglected. Assumption (a) corresponds to random spacing of objects in one “ping”, and movement of the objects to the next “ping” [21,10]. Assumption (b) means that only echoes backscattered directly from the objects are significant, so that those backscattered via other objects (second-order effects) can be ignored [31,22,10]. Assumption (c) may be a reasonable approximation except for strong scatterers at high densities, distributed over an extended volume [32,22,33].

For a multitude of small objects in the sampled volume, the echoes from individual objects cannot be resolved, but combine to form a received signal with varying amplitude. The echo intensity is still a measure of the biomass in the volume [6,7,10]. Under the above assumptions the total echo intensity is the incoherent sum of the individual echo intensities [22]. The volume backscattering coefficient s_v is the backscattering cross section per unit volume [21]. Consequently, the volume backscattering coefficient can be calculated as a sum over backscattering cross sections (i.e., intensities) per unit volume [21,34], so that

$$s_v \equiv \lim_{\Delta V \rightarrow 0} \left(\sum_{j=1}^N N_j \sigma_{bs,j} \right) = \lim_{\Delta V \rightarrow 0} \left(\frac{1}{\Delta V} \sum_{j=1}^N m_j \sigma_{bs,j} \right), \quad (32)$$

where N is the number of scattering object types, $N_j = m_j / \Delta V$ is the number of scattering objects of type j per volume ΔV , m_j is the number of scattering objects of type j in the volume ΔV , and $\sigma_{bs,j}$ is the backscattering cross section for an object of type j , $j = 1, \dots, N$. From Eq. (32), $m_j \sigma_{bs,j}$ represents the total backscattering cross section for scatterers of type j , in the volume ΔV . Consequently,

$$\Delta \sigma_{bs} \equiv \sum_{j=1}^N m_j \sigma_{bs,j} \quad (33)$$

represents the total backscattering cross section over all scatterer types, in the volume ΔV . From Eqs. (32) and (33) it follows that $s_v = \lim_{\Delta V \rightarrow 0} (\Delta \sigma_{bs} / \Delta V) \equiv d\sigma_{bs} / dV$, so that

$$d\sigma_{bs} = s_v dV. \quad (34)$$

From Eq. (33) it is seen that $d\sigma_{bs}$ represents backscattering from a multitude of objects in the unit volume dV , including objects of different types, and objects of the same type with different sizes.

As explained above, Eqs. (29) and (31) apply not only to a single scattering object in the far field, but also to a multitude of far-field objects of different types, materials and sizes, confined to a sufficiently small volume in space, so that the backscatter at the transducer appears as coming from a single point (target) in the far field. For backscattering from the small unit volume dV in V_{obs} , Eq. (29) thus yields

$$d\Pi_R = \Pi_T \cdot F_{\Pi} \cdot G^2(\theta, \varphi) \cdot \frac{\lambda^2}{(4\pi)^2} \cdot \frac{e^{-4\alpha r}}{r^4} \cdot d\sigma_{bs} \quad (35)$$

for the received electrical power.

Now, assume uniform distribution of scattering objects in the volume V_{obs} , so that $d\sigma_{bs}$ as given by Eq. (34) can be used everywhere in V_{obs} , meaning that backscatter is essentially the same for objects anywhere in the transducer beam [22]. Integration of Eq. (35) over this volume, and substitution of Eq. (34), yields

$$\Pi_R = \int_{V_{obs}} \Pi_T \cdot \frac{\lambda^2}{(4\pi)^2} \cdot \frac{e^{-4\alpha r}}{r^4} \cdot F_{\Pi} \cdot G^2(\theta, \varphi) \cdot s_v dV, \quad (36)$$

where $dV = r^2 dr d\Omega$.

The present continuous-wave analysis applies also to the steady-state portion of transient signals. Assume the observation volume V_{obs} in the far field is insonified using a tone burst (a pulsed sinusoidal ‘‘ping’’) of time duration τ_p and angular carrier frequency ω . The spatial extension of the pulse is $c_0\tau_p$. Assume $c_0\tau_p \ll r_{\max} - r_{\min}$. Within the spherical shell volume V_{obs} , the tone burst will then cover a spherical shell subvolume, V_p (here denoted ‘‘ping volume’’), contained within ranges, say, r_{p1} and r_{p2} . Consider backscatter from V_p . At the transducer, the arrival times of the start and stop of the tone burst are $2r_{p1}/c_0$ and $2r_{p2}/c_0$, respectively. By defining $dr_p \equiv r_{p2} - r_{p1}$ as the thickness of the spherical shell volume V_p , one gets $dr_p = \frac{1}{2}c_0\tau_p$. Consequently, $dV = \frac{1}{2}c_0\tau_p \cdot r^2 d\Omega$. Substitution of this expression into Eq. (36) leads to

$$\frac{\Pi_R}{\Pi_T} = F_{\Pi} \cdot \frac{\lambda^2}{(4\pi)^2} \cdot \frac{e^{-4\alpha r}}{r^2} \cdot \frac{c_0\tau_p}{2} \cdot s_v \cdot \int_{4\pi} G^2(\theta, \varphi) d\Omega \quad (37)$$

for the transmit-receive electrical power transfer function due to volume backscattering from V_p , where $r \approx (r_{p1} + r_{p2})/2$. Note that at this stage of the derivation, integration over range r in the finite volume V_{obs} has not been carried out. This is treated in Section 5.

3.2 Volume backscattering coefficient

By rearranging Eq. (37) to solve for the volume backscattering coefficient, s_v , one obtains

$$s_v = \frac{32\pi^2 \cdot r^2 \cdot e^{4\alpha r} \cdot \Pi_R}{G_0^2 \cdot \psi \cdot \lambda^2 c_0 \cdot \tau_p \cdot F_{\Pi} \cdot \Pi_T}, \quad (38)$$

where

$$\psi \equiv \int_{4\pi} |\mathbf{B}_i(\theta, \varphi)|^4 d\Omega = \frac{1}{G_0^2} \int_{4\pi} G^2(\theta, \varphi) d\Omega, \quad (39)$$

$$G_0 \equiv G(0,0) = \eta \cdot D, \quad (40)$$

are the equivalent two-way solid beam angle of the transducer [21] and the axial transducer gain, respectively. The latter of the two expressions given in Eq. (39) follows from Eqs. (24) and (40).

Eq. (37), or equivalently, Eq. (38), is the electroacoustic power budget equation for volume backscattering from a thin spherical shell subvolume V_p (the ‘‘ping volume’’) of thickness $dr_p = \frac{1}{2} c_0 \tau_p$ in the observation volume V_{obs} , under small-amplitude (linear) sound propagation conditions.

4 Formulation in terms of echo integration

The above continuous-wave analysis applies to each frequency component of a finite duration sonar signal. It applies approximately also to long tone bursts with angular carrier frequency ω , such as typical fisheries echosounder signals. From Eqs. (17) and (28), the transmitted and received electrical powers are given as, at the angular frequency ω ,

$$\Pi_T = \frac{R_T}{|\mathbf{Z}_T|^2} \cdot (V_T^{rms})^2, \quad \Pi_R = \frac{R_E}{|\mathbf{Z}_E|^2} \cdot (V_R^{rms})^2. \quad (41)$$

where $V_T^{rms} = |\mathbf{V}_T|/\sqrt{2}$ and $V_R^{rms} = |\mathbf{V}_R|/\sqrt{2}$ are the effective (rms) amplitudes of the transmitted and received voltage signals $V_T(t)$ and $V_R(t)$, respectively, at the transducer terminals.

In reality, for a multitude of scattering objects in the sampling volume, the received voltage signal $V_R(t)$ is the sum of received echoes, with a strongly time-varying amplitude due to interference of overlapping echoes. In oceanic surveys, echo integration processing is commonly used, based on measured voltage amplitudes [22,10], where signals are received

and integrated over a gate opening time. It is thus of interest to formulate Eqs. (31) and (38) in terms of echo integration of $V_T(t)$ and $V_R(t)$. Following refs. [21,22], two different cases of echo integration are discussed: (a) “short ping and long gate” ($\tau_p \ll \tau_g$), and (b) “long ping and short gate” ($\tau_p \gg \tau_g$). Here, τ_p and $\tau_g \equiv t_{g2} - t_{g1}$ are, respectively, the “ping duration” and the “gate opening time”, where t_{g1} and t_{g2} are the times of gate opening and closing, respectively. Thus, in both cases the backscattered voltage signal is now integrated over a time period t_{g1} to t_{g2} , corresponding to backscattering from a thin spherical shell volume V_g (denoted “gated volume”), contained within ranges r_{g1} and r_{g2} . Consequently, $t_{g1} = 2r_{g1}/c_0$ and $t_{g2} = 2r_{g2}/c_0$. By defining $dr_g \equiv r_{g2} - r_{g1}$, the thickness and range of V_g are $dr_g = \frac{1}{2}c_0\tau_g$ and $r \approx (r_{g1} + r_{g2})/2$, respectively.

4.1 Echo integration using “short ping and long gate” ($\tau_p \ll \tau_g$)

Consider an echo integration approach where the duration of the ping, τ_p , is taken to be very small compared with the gate opening time τ_g that selects the shell thickness dr_g of the volume V_g , i.e. $\tau_p \ll \tau_g$ [21,22].

Assume that the electrical impedance ratios $R_T/|Z_T|^2$ and $R_E/|Z_E|^2$ are approximately constant within the narrow frequency band of the transmitted and received voltage signals $V_T(t)$ and $V_R(t)$. From Eqs. (41), the average transmitted and received electrical powers [35] can then be calculated approximately in terms of the squared effective amplitudes of the transmitted and received voltage waveforms, respectively, averaged over time periods corresponding to the gate opening time, τ_g , giving

$$\Pi_T \approx \frac{R_T}{|Z_T|^2} \cdot \frac{1}{\tau_g} \int_0^{\tau_g} |V_T(t)|^2 dt = \frac{R_T}{|Z_T|^2} \cdot \frac{1}{\tau_p} \int_0^{\tau_p} |V_T(t)|^2 dt = \frac{R_T}{|Z_T|^2 \tau_p} \cdot [tivs]_T, \quad (42)$$

$$\Pi_R \approx \frac{R_E}{|Z_E|^2} \cdot \frac{1}{\tau_g} \int_{t_{g1}}^{t_{g2}} |V_R(t)|^2 dt = \frac{R_E}{|Z_E|^2 \tau_g} \cdot [tivs]_R^{GV}, \quad (43)$$

where

$$[tivs]_T \equiv \int_0^{\tau_p} |V_T(t)|^2 dt, \quad [tivs]_R^{GV} \equiv \int_{t_{g1}}^{t_{g2}} |V_R(t)|^2 dt, \quad (44)$$

are defined as the “time-integral-voltage-squared” $[tivs]$ values of the waveforms $V_T(t)$ and $V_R(t)$, respectively. Insertion in Eqs. (31) and (38) yields

$$\sigma_{bs} = \frac{16\pi^2 \cdot r^4 \cdot e^{4\alpha r} \cdot \tau_p \cdot [tivs]_R^{GV}}{G^2(\theta, \varphi) \cdot \lambda^2 \cdot F_{VV}^2 \cdot \tau_g \cdot [tivs]_T} , \quad (45)$$

$$s_v = \frac{32\pi^2 \cdot r^2 \cdot e^{4\alpha r} \cdot [tivs]_R^{GV}}{G_0^2 \cdot \psi \cdot \lambda^2 c_0 \cdot \tau_g \cdot F_{VV}^2 \cdot [tivs]_T} , \quad (46)$$

respectively, for the single-target backscattering cross section and the volume backscattering coefficient.

4.2 Echo integration using “long ping and short gate” ($\tau_p \gg \tau_g$)

Consider an alternative echo integration approach where the gate opening time τ_g that selects the shell thickness dr_g of the volume V_g , is taken to be very small compared with the ping duration τ_p , i.e. $\tau_p \gg \tau_g$ [21].

In this case, and under the same electrical impedance assumptions as above for a narrowband sonar ping, the average received electrical power is still given as in Eq. (43), whereas the transmitted electrical power, averaged over a time period corresponding to the gate opening time, τ_g , is given from Eq. (41) as

$$\Pi_T \approx \frac{R_T}{|Z_T|^2} \cdot \frac{1}{\tau_g} \int_0^{\tau_g} |V_T(t)|^2 dt = \frac{R_T}{|Z_T|^2 \tau_g} \cdot [tivs]_T^{GV} , \quad (47)$$

where

$$[tivs]_T^{GV} \equiv \int_0^{\tau_g} |V_T(t)|^2 dt , \quad (48)$$

is the “time-integrated-voltage-squared” values of $V_T(t)$, integrated over the gate opening time τ_g (which in this case is much shorter than the duration of $V_T(t)$, τ_p). Insertion in Eqs. (31) and (38) yields

$$\sigma_{bs} \approx \frac{16\pi^2 \cdot r^4 \cdot e^{4\alpha r} \cdot [tivs]_R^{GV}}{G^2(\theta, \varphi) \cdot \lambda^2 \cdot F_{VV}^2 \cdot [tivs]_T^{GV}} , \quad (49)$$

$$s_v \approx \frac{32\pi^2 \cdot r^2 \cdot e^{4\alpha r} \cdot [tivs]_R^{GV}}{G_0^2 \cdot \psi \cdot \lambda^2 c_0 \cdot \tau_p \cdot F_{VV}^2 \cdot [tivs]_F^{GV}}, \quad (50)$$

respectively, for the single-target backscattering cross section and the volume backscattering coefficient.

5 Implications for the echo-integrator equation

s_v , as given by Eqs. (46) or (50) for the two different cases of echosounder operation, respectively, represents the volume backscattering from a thin spherical shell subvolume V_g (the “gated volume”) of thickness $dr_g = \frac{1}{2} c_0 \tau_g$ in the observation volume V_{obs} , weighted in angular direction (θ, φ) by the transducer’s transmit and receive beam patterns, $\mathbf{B}_i(\theta, \varphi)$. The angular weighing is accounted for by the equivalent two-way solid beam angle, ψ .

The volume backscattering from the finite spherical shell volume V_{obs} , between ranges r_{\min} and r_{\max} , is obtained by measuring s_v for a continuous sequence of gated volumes, V_g , and integrating s_v over the range of these gated volumes, giving the area backscattering coefficient [18,36]

$$s_a \equiv \int_{r_{\min}}^{r_{\max}} s_v dr, \quad (51)$$

representing the backscattering cross section per unit area (dimensionless), within V_{obs} . In echosounder output, s_a is frequently given in terms of [18,36,10]

$$s_A \equiv 4\pi \cdot 1852^2 \cdot s_a, \quad (52)$$

where s_a has been multiplied by the surface area of a sphere with radius one nautical mile. s_A is denoted the nautical area scattering coefficient (NASC) [36]. The density of targets, expressed as the number of specimens contained in V_{obs} per square nautical mile, is then given as [36]

$$\rho_a = \frac{s_A}{4\pi \langle \sigma_{bs} \rangle} = \frac{1852^2 \cdot s_a}{\langle \sigma_{bs} \rangle}. \quad (53)$$

Insertion of Eqs. (51), (46) and (50) into Eq. (53) yields

$$\rho_a = \frac{C}{\psi \langle \sigma_{bs} \rangle} E \quad , \quad (54)$$

where

$$E \equiv \int_{r_{\min}}^{r_{\max}} r^2 e^{4\alpha r} [tivs]_R^{GV} dr \quad , \quad (55)$$

and

$$C \equiv \begin{cases} \frac{32\pi^2 \cdot 1852^2}{G_0^2 \cdot \lambda^2 c_0 \cdot \tau_g \cdot F_{VV}^2 \cdot [tivs]_T} \quad , & \tau_p \ll \tau_g \quad (\text{"short ping and long gate"}) \\ \frac{32\pi^2 \cdot 1852^2}{G_0^2 \cdot \lambda^2 c_0 \cdot \tau_p \cdot F_{VV}^2 \cdot [tivs]_T^{GV}} \quad , & \tau_p \gg \tau_g \quad (\text{"long ping and short gate"}) \end{cases} \quad (56)$$

Eq. (54) is recognized as the echo-integrator equation, Eq. (1), with $\bar{g}=1$ (no TVG correction) [37]. C is the calibration factor of Eq. (1), which is given for two different cases of echosounder operation and processing. E is the echo-integral for the observation volume V_{obs} . For each gated volume V_g in V_{obs} , the term $r^2 e^{4\alpha r}$ is the usual " $20\log(r) + 2\hat{\alpha}r$ " TVG factor for volume backscattering. $[tivs]_R^{GV}$ is the time integrated received signal (echo), over the time interval τ_g , averaged over many transmissions. $[tivs]_T$ and $[tivs]_T^{GV}$ represent two different time integrations of the transmitted signal, integrated over the time intervals τ_p and τ_g , respectively.

Eqs. (54)-(56) thus represent a functional relationship for the abundance estimation, where the calibration factor C of Eq. (1) is now given fully in terms of the echosounder parameters.

6 Discussion

6.1 Consistency with and generalization of previous work

The electroacoustic power budget equation for single-target backscattering is used in on-ship calibration of scientific echosounders using solid spheres [20], and the electroacoustic power budget equation for volume backscattering is used in oceanic surveys, for echo integration related to abundance estimation of fish and zooplankton [18,19], and for species identification [38-40]. Consistency of the key equations resulting from the present work, Eqs. (31) and (38), Eqs. (45) and (46), Eqs. (49) and (50), and Eqs. (54)-(56), with previous work in the field, is essential.

Eqs. (31) and (38) are equal to the expressions derived by Simrad [18], and used by Korneliussen [19] and Simmonds and MacLennan [10], with the exception that the electrical impedance factor F_{Π} was not included or addressed by those authors, which means that their expressions are valid for $F_{\Pi} = 1$. Eqs. (31) and (38) were also derived by Pedersen [11], who

seems to have been the first to include the electrical impedance factor F_{Π} in the equations. The present analysis is more detailed than the one given by Pedersen, with correction of some minor irregularities in that derivation, also extending the analysis to account for echo integration, and formulations in terms of an echo integrator equation.

Ona *et al.* [20] used a logarithmic variant of Eqs. (31) and (38). The factor F_{Π} was not included or addressed. An additional term $S_{a,corr}$ was included in their expression corresponding to Eq. (38), denoted “integration correction”, and used as a correction to the nominal pulse duration, τ_p . In this context it is of interest to note that Eq. (38) involves the “ping duration” τ_p , whereas Eq. (46) involves the “gate opening time” τ_g , where $\tau_g \gg \tau_p$. Possible erroneous use of τ_p instead of τ_g in Eq. (46), would require a large correction factor τ_g/τ_p in the denominator of Eq. (46).

Eqs. (45) and (46), and Eqs. (49) and (50), represent further development of the equations presented by Simrad [18] (used e.g. by [19,10,17,20]), and Pedersen [11], represented here by Eqs. (31) and (38), to express these equations for single-target and volume backscattering in terms of voltage echo integration ([*tivs*]) processing instead of electrical power, for two cases of echo integration, “short ping and long gate” and “long ping and short gate”, respectively. It is noted that the relevant electrical impedance factor for the echo integration ([*tivs*]) formulation is F_{VV}^2 , and that the expressions involve τ_p or τ_g , or both, depending on which echo integration approach is being used.

The two echo integration formulations for σ_{bs} and s_v described in Section 4.1 and 4.2, involve time integration parameters which in general are different from the conventional formulations in terms of electrical powers, Eqs. (31) and (38), and also different from one method of echo integration to the other.

For the “short ping and long gate” echo integration method ($\tau_p \ll \tau_g$), the ratio of the ping duration to the gate opening time, τ_g/τ_p , appears explicitly in the expression for σ_{bs} , cf. Eq. (45). In the corresponding expression for σ_{bs} given in terms of electrical powers, Eq. (31), τ_p and τ_g are not explicitly involved. In the echo integration expression for s_v , Eq. (46), τ_g is shown to be the relevant integration time parameter, whereas in the corresponding expression given in terms of electrical powers, Eq. (38), τ_p is the time parameter involved.

For the “long ping and short gate” echo integration ($\tau_p \gg \tau_g$), the relevant time parameters are quite different. In this case, τ_p and τ_g are not explicitly involved in the expression for σ_{bs} , cf. Eq. (49), as for the corresponding expression given in terms of electrical power, Eq.

(31). In the expression for s_v , Eq. (50), the time integration parameter explicitly involved is τ_p , as for the corresponding expression in terms of electrical power, Eq. (38).

In a time domain analysis, Clay and Medwin [21] derived two expressions for the “in-water” acoustic power budget equation, applicable to the two cases of echosounder operation, “short ping and long gate” and “long ping and short gate”, respectively, cf. Appendix B. A similar “in-water” acoustic power budget equation, applicable to the case “short ping and long gate”, was derived by Medwin and Clay [22], also based on a time domain analysis. A comparison of “in-water” acoustic power budget equations derived from Eq. (13) for these two cases, Eqs. (B.5), and the acoustic power budget equations given by Clay and Medwin [21,22], given by Eqs. (B.2) and (B.3), respectively, reveals that the respective equations for “short ping and long gate” and “long ping and short gate” are basically equal (except for fluid absorption, which was not accounted for in Clay and Medwin’s [21] theory). The integration over a multitude of scattering objects performed above is similar to the integration made by Clay and Medwin [21,22], although the approaches and mathematical details are quite different. Clay and Medwin’s [21] and Medwin and Clay’s [22] analyses were carried out in the time domain, using a transmitted pressure pulse (“ping”) of duration τ_p and integrating over a gate opening time, τ_g , whereas the present analysis is a frequency domain analysis, adapted to a time domain echo integration formulation, cf. Appendix B. Eqs. (B.2)-(B.5) show that the methodologies used and results obtained in the present analysis, as compared with Clay and Medwin’s [21] and Medwin and Clay’s [22] analyses, are consistent.

Moreover, in Appendix B it is also shown that Eqs. (45) and (46) for σ_{bs} and s_v represent an extension of the “in-water” s_v expressions given by Clay and Medwin [21,22] for “short ping and long gate”, based on [tips] processing, to account for the transducer and electronics components of the echosounder system, using [tivs] processing. Eqs. (49) and (50) represent a similar extension of the “in-water” s_v expression given by Medwin and Clay [22] for “long ping and short gate”.

6.2 Electrical impedance factors, F_{Π} and F_{VV}^2

It is noted that different electrical impedance factors are involved for the continuous-wave and echo integration ([tivs]) formulations of the electroacoustic power budget equations. The electrical impedance factors involved are F_{Π} and F_{VV}^2 , given by Eqs. (30) and (27a), respectively. These represent the effect of electrical termination load, in terms of the electrical impedances of the transducer and the electrical termination network. F_{Π} applies to the continuous-wave formulations given in terms of electrical powers, Eqs. (31) and (38), whereas F_{VV}^2 applies to the echo integration ([tivs]) formulations, cf. Eqs. (45) and (46), Eqs. (49) and (50), and Eqs. (54)-(56). Certain cases of electrical matching may be of particular interest, such as $\mathbf{Z}_E = \mathbf{Z}_R^*$, $\mathbf{Z}_E = \mathbf{Z}_R$, $|\mathbf{Z}_E| \gg |\mathbf{Z}_R|$, and $|\mathbf{Z}_E| \ll |\mathbf{Z}_R|$.

If Z_E is chosen equal to Z_R^* (“*” denotes complex conjugate), to maximize the power transfer from the transducer upon signal reception, one has $F_{\Pi} \approx R_T/R_R$ and $F_{VV}^2 \approx (R_T/|Z_T|)^2$. If in addition $R_R = R_T$, F_{Π} becomes equal to 1. In practice, measurement of Z_R may not be readily available, but Z_R is often assumed to be equal to Z_T , in which case $F_{\Pi} = 1$ is automatically fulfilled over the frequency band for which $Z_E = Z_R^*$ is achieved. F_{VV}^2 approaches 1 when the transducer’s electrical reactance $X_T \approx 0$, i.e., in a frequency band around a series resonance frequency of the transducer.

If Z_E is chosen equal to Z_R e.g. to minimize reflections, one has $F_{\Pi} \approx R_T R_R / |Z_R|^2$ and $F_{VV}^2 \approx (R_T/|Z_T|)^2$. If the usual assumption $Z_R = Z_T$ is made, one obtains $F_{\Pi} \approx (R_T/|Z_T|)^2$, so that both F_{Π} and F_{VV}^2 approach 1 when the electrical reactance $X_T \approx 0$, cf. above.

In other cases a high value of Z_E may be chosen, $|Z_E| \gg |Z_R|$ (approximately open circuit), to maximize the voltage V_R across the receiver terminals instead of the transferred electrical power. In this case $F_{\Pi} \approx 4R_T R_E / |Z_E|^2 \approx 4R_R R_E / |Z_E|^2 \ll 1$, where the assumption $R_R = R_T$ has been made. Similarly, $F_{VV}^2 \approx (2R_T/|Z_T|)^2$ which approaches 4 when the electrical reactance $X_T \approx 0$, cf. above.

If a small value of Z_E is chosen, $|Z_E| \ll |Z_R|$ (approximately short circuit), to maximize the current I_R across the receiver terminals, one again obtains $F_{\Pi} \approx 4R_T R_E / |Z_R|^2 \approx 4R_R R_E / |Z_R|^2 \ll 1$, where the assumption $R_R = R_T$ has been made. In this case $F_{VV}^2 \approx (2R_T |Z_E| / |Z_R| |Z_T|)^2 \ll 1$.

In practice F_{Π} (or F_{VV}^2) has not been accounted for in the power budget equations used in echosounder calibration and oceanic surveys [18,19,10,17,20]. This corresponds to setting F_{Π} equal to 1. From the above analysis, this is valid only for electrical termination conditions for which $Z_E = Z_R^*$, or for $Z_E = Z_R$ when $X_T = 0$.

For electrical impedance matching situations for which F_{Π} (or F_{VV}^2) is not equal to 1 (cf. above), the error introduced by disregarding the electrical impedance factor may in practice be cancelled by on-ship calibration of the echosounder, provided that no sonar parameter setting is changed from calibration to survey operation, and that the performance of the system remains unchanged (e.g., unchanged temperature).

In situations where transducer and sonar parameters *do* change from calibration to survey operation, the performance of the system is changed, and compensation for such changes may

be warranted. For example, a difference in sea temperature from calibration site to survey operation, as addressed by [17], may cause a shift in the transducer frequency response, leading to a shift in the echosounder system gain. Temperature may influence on the electrical impedances of the transducer ($\mathbf{Z}_T, \mathbf{Z}_R$) and the receive electronics (\mathbf{Z}_E), the beam pattern ($\mathbf{B}_i(r, \theta, \varphi)$), and thus on the equivalent two-way solid beam angle (ψ) and the transducer gain ($G(\theta, \varphi)$). If the total gain shift is not compensated for, a bias in the fish abundance estimate may result. A compensation method needs to account for the factors F_{Π} or F_{VV} , depending on the signal detection and processing approach used in the system. The expressions given here, Eqs. (31) and (38), Eqs. (45) and (46), Eqs. (49) and (50), and Eqs. (54)-(56), accounting for F_{Π} and F_{VV} , provide functional relationships to enable compensation for change of sonar parameters from calibration to survey operation.

6.3 Transducer gain, $G(\theta, \varphi)$

The transducer gain $G(\theta, \varphi)$ is defined by Eq. (24). From Eqs. (24), (19), (5) and (2), it can also be written as

$$G(\theta, \varphi) = \frac{I_i(r, \theta, \varphi) \cdot 4\pi r^2 \cdot e^{2\alpha r}}{\Pi_T} . \quad (57)$$

From Eq. (57), $G(\theta, \varphi)$ is interpreted as the ratio of the absorption-corrected transmitted acoustic power radiated in the (θ, φ) direction (i.e., under lossless conditions in the fluid), to the transmitted electrical power. That is, $G(\theta, \varphi)$ can be interpreted as the transducer's one-way electroacoustic "efficiency" during transmission (or reception), for radiation (or reception) in the (θ, φ) direction, under lossless conditions in the fluid. In other words, $G(\theta, \varphi)$ is either (a) a measure of how well the transducer converts input electrical power into acoustic intensity transmitted in a specific direction, (θ, φ) , or (b) *vice versa*, converts acoustic intensity received from a specific direction, (θ, φ) , into electrical power, where both (a) and (b) are related to lossless conditions in the fluid. In particular, the axial reception transducer gain G_0 , given by Eq. (40), represents the transducer's one-way electroacoustic "efficiency" at the beam axis during transmission (or reception), under small-amplitude (linear) and lossless conditions in the fluid.

Hence, for a transmit-receive system, the products $G(\theta, \varphi) = \sqrt{G(\theta, \varphi)} \sqrt{G(\theta, \varphi)}$ and $G_0 = \sqrt{G_0} \sqrt{G_0}$ may represent the transducer's two-way electroacoustic "efficiency" in the (θ, φ) and axial directions, respectively, under lossless and small-amplitude conditions in the fluid medium.

Since η and D are both independent of (θ, φ) , it follows from Eq. (24) that

$$\eta = \frac{1}{4\pi} \int_{4\pi} G(\theta, \varphi) d\Omega, \quad (58)$$

which supports the above interpretation of $G(\theta, \varphi)$.

6.4 Assumptions underlying the analysis

A number of assumptions are used to derive the equations for the backscattering cross section, σ_{bs} , and the volume backscattering coefficient, s_v , cf. Eqs. (31) and (38), Eqs. (45) and (46), Eqs. (49) and (50), leading to Eqs. (54)-(56). Such assumptions include:

- (a) the sound pressure amplitudes are sufficiently small to avoid finite amplitude effects in the sea (i.e., linearized theory of sound propagation applies),
- (b) the electrical voltage transmit amplitude is sufficiently small to avoid finite amplitude effects in the electroacoustic transducer (i.e., the transducer is linear),
- (c) the transducer is passive and reciprocal,
- (d) the electrical impedances of the transducer and receiving electronics are approximately constant in the narrow frequency band of a sonar ping,
- (e) targets are in the far field of the transducer,
- (f) the volume backscattering coefficient can be calculated as a sum of backscattering cross sections (i.e., intensities) per unit volume,
- (g) the scattering objects are uniformly distributed in the observation volume, with
- (h) random phases of the scattered echoes (i.e., random spacing of scattering objects, and movement of objects from one transmission to the next),
- (i) possible multiple-scattering effects and interaction between objects are neglected, and
- (j) excess attenuation from power extinction caused by volume scattering is neglected.

Assumptions (b)-(d) relate to the transducer and electric components of the echosounder system. For the “in-water” part of the analysis, assumptions (e)-(j) are included in the set of assumptions used by Clay and Medwin [21] and Medwin and Clay [22] to derive the analogous “in-water” expressions for s_v , accounting for acoustic pressure only.

The discussion of the validity of these assumptions is an extensive and complex subject, beyond the scope of the present work. An objective is however to clearly point out the assumptions which are used, and at which step in the derivation each of them is applied. Relatively extensive discussions on the validity of “in-water” assumptions (e)-(j) used here are given by Medwin and Clay [22] and Simmonds and MacLennan [10], also summarizing key literature in the field.

The influence of finite amplitude (nonlinear sound propagation) effects, which is not covered by the mentioned literature, related to assumption (a), is addressed elsewhere [11-16].

7 Conclusions

Electroacoustic power budget equations and the echo-integrator equation are routinely used in calibration and oceanic surveys for fish abundance estimation and species identification using scientific echosounders. These equations constitute the fundament for international regulations of marine resources. It is documented that scientific fisheries echosounders have been and are operated under conditions of finite amplitude (nonlinear) sound [11-16], with erroneous measurements as a consequence. Control with and correction for sea temperature or finite amplitude effects demands the calibration factor C of the echo-integrator equation to be fully known in terms of echosounder system parameters. Such a functional relationship for C is however not available from earlier literature.

In the present work, the theoretical basis for the power budget and echo-integrator equations is revisited, and an expression for C is derived from fundamental acoustical principles, cf. Eq. (56). The objective has been (1) to provide a derivation of these equations for integration in a more complete functional relationship for abundance measurements, where the calibration factor C of the traditional echo-integrator equation is specified fully in terms of a functional relationship accounting for the sonar system's electrical and acoustical parameters, (2) to extend previous theory to account for more general conditions of electrical termination, (3) to formulate the expressions in terms of voltage signal echo integration processing, and (4) thereby generalize the Clay-Medwin [21,22] formulations based on echo integration of "in-water" sound pressure signals, to account for the transducer and electronics components of the echosounder system, in formulations based on echo integration of voltage signals.

As part of this analysis, two electroacoustic power budget equations are derived, for single-target and volume backscattering in the far field, respectively. These are formulated in terms of the backscattering cross section, σ_{bs} (single-target backscattering, used in echosounder calibration), and the volume backscattering coefficient, s_v (multiple-target volume backscattering, used in oceanic surveys), cf. Eqs. (31) and (38), respectively. σ_{bs} and s_v are determined by the transmitted and received electrical powers measured at the transducer's electrical port, properties of the transmitted and scattered sound fields, properties of the fluid medium, the electrical impedances of the transducer at transmission and reception, and the electrical impedance of the electrical termination. In addition to the continuous-wave expressions given by Eqs. (31) and (38), echo-integration formulations of these power budget equations are derived, more clearly related to the actual echosounder signal processing. Two cases of echosounder operation and processing are considered: "short ping and long gate", and "long ping and short gate", cf. Eqs. (45)-(46) and Eqs. (49)-(50), respectively.

The resulting formulations of the electroacoustic power budget equation for volume backscattering, Eqs. (38), (46) and (50), are shown to be valid for distributions of different type scattering objects, or the same type with different sizes, located at arbitrary positions in the far field in a homogeneous medium.

A derivation or documentation of these equations for conditions of acoustic wave propagation, does not seem to have been previously available in published literature.

The results given here represent an extension of the “in-water” sound pressure based expressions for the volume backscattering coefficient s_v given by Clay and Medwin [21,22], to account for the electronics and transducer parts of the sonar system. The results represent an extension of other previous work [18,19,10,11] related to the backscattering cross section, σ_{bs} , and the volume backscattering coefficient, s_v , by accounting for (a) arbitrary electrical termination upon signal reception, (b) time domain voltage echo integration processing, and (c) two modes of echosounder operation and processing. The results are otherwise fully consistent with these earlier results. It is shown under which conditions of electrical termination the previously derived electroacoustic power budget equations are valid. Consequently, the present theory connects the acoustic power budget equations derived by Clay and Medwin [21,22], based on an “in-water” time-domain analysis, to the electroacoustic power budget equations given by Simrad and others [18,19,11], based on a frequency-domain approach. Use of the expressions derived here do not require other measurements than those already made in conventional fish abundance estimation.

The equations derived here, Eqs. (54)-(56), represent a more complete functional relationship for acoustic abundance estimation than the traditional echo-integrator equation, Eq. (1), which is based on a calibration factor, C . In the present analysis, C is determined in terms a mathematical expression accounting for the sonar system’s electrical and acoustical parameters, cf. Eq. (56). The formulation given here constitutes a necessary basis for evaluation and correction of certain measurement errors in abundance estimation and species determination, such as due to possible changes in sea temperature from calibration to survey operation, or finite amplitude (nonlinear) sound propagation effects in seawater (not accounted for in the present analysis) [11,16]. Moreover, the functional relationship given here enables study of the influence of other parameters and conditions involved in calibration and oceanic surveying, in terms of sensitivity, uncertainty and error analyses.

Acknowledgement

The authors wish to acknowledge Magne Vestheim, University of Bergen, Dept. of Physics and Technology, Norway, for useful discussions related to topics addressed here.

References

- ¹ O. Nakken and Ø. Ulltang, "A comparison of the reliability of acoustic estimates for fish stock abundance and estimates obtained by other assessment methods in Northeast Atlantic", *FAO Fish. Rep.* **300** (1983), pp. 249-260.
- ² D. N. MacLennan, "Acoustical measurements of fish abundance", *J. Acoust. Soc. Am.* **87**(1), 1-15 (1990).
- ³ C. S. Clay and H. Medwin, *Acoustical oceanography: Principles and applications*, J. Wiley & Sons, New York (1977), 544 p.

- ⁴ H. Medwin and C. S. Clay, *Fundamentals of acoustical oceanography*, Academic Press, Boston (1998), 712 p.
- ⁵ J. Simmonds and D. N. MacLennan, *Fisheries acoustics*, 2nd ed., Blackwell Science Ltd., Oxford, UK (2005), 437 p.
- ⁶ O. Dragesund and S. Olsen, "On the possibility of estimating year-class strength by measuring echo-abundance of 0-group fish", *Fiskeridirektoratets Skrifter, Serie Havundersøkelser*, **13**(8) (1965), pp. 48-75.
- ⁷ J. Dalen and O. Nakken, "On the application of the echo integration method", *ICES Document CM 1983/B:19* (1983), 30 p.
- ⁸ K. G. Foote, "Optimizing copper spheres for precision calibration of hydro acoustic equipment", *J. Acoust. Soc. Am.* **71**, 742–747 (1982).
- ⁹ K. G. Foote, H. P. Knudsen, G. Vestnes, D. N. MacLennan, and E. J. Simmonds, "Calibration of acoustic instruments for fish density estimation. A practical guide", *ICES Cooperative Research Report No. 144*, International Council for the Exploration of the Sea, Copenhagen, Denmark (1987), 81 p.
- ¹⁰ Ref. [5], pp. 59-60, 110, 120-121, 187-191, and 197.
- ¹¹ A. Pedersen, "Effects of nonlinear sound propagation in fisheries research", Ph.D. thesis, University of Bergen, Dept. of Physics and Technology, Bergen, Norway (2006), 307 p.
URL: https://bora.uib.no/handle/1956/2158?mode=full&submit_simple>Show+full+item+record (last viewed: Dec. 24, 2013).
- ¹² A. C. Baker and P. Lunde, "Nonlinear propagation from circular echo-sounder transducers. Numerical simulation results", *CMR Technical Note CMR-TN01-A10010-rev-01*, Christian Michelsen Research AS, Bergen, Norway (August 2011), 23 p. De-classified revision of *CMR Technical Note CMR-TN01-F10010* (February 2001) (confidential), 22 p.
- ¹³ A. C. Baker and P. Lunde, "Nonlinear effects in sound propagation from echo-sounders used in fish abundance estimation. Numerical simulation results", *CMR Technical Note CMR-TN02-A10008-rev-01*, Christian Michelsen Research AS, Bergen, Norway (August 2011), 27 p. De-classified revision of *CMR Technical Note CMR-TN02-F10008* (April 2002) (confidential), 26 p.
- ¹⁴ F. E. Tichy, H. Solli and H. Klaveness, "Nonlinear effects in a 200-kHz sound beam and consequences for target strength measurement", *ICES Journal of Marine Science* **60**, 571-574 (2003).
- ¹⁵ "Nonlinear effects: Recommendation for fishery research investigations". On URL: <http://www.simrad.com/www/01/nokbg0240.nsf/AllWeb/F176A291CB3E64CBC12578E800491241?OpenDocument> (date last viewed Dec. 24, 2013). Revised version of *Simrad News Bulletin*, Simrad AS (now Kongsberg Maritime AS), Horten, Norway (March 2002), 2 p.
- ¹⁶ P. Lunde and A. O. Pedersen, "Sonar and power budget equations for backscattering of finite amplitude sound waves, with implications in fishery acoustics for abundance estimation of marine resources", in U. Kristiansen (ed.), *Proc. of 35th Scandinavian Symposium on Physical Acoustics, Geilo, Norway, January 29 - February 1, 2012*, Norwegian Physical Society, 11 p. (ISBN 978-82-8123-012-5). Available at URL <http://www.ntnu.edu/sspa> (last viewed Dec. 24, 2013).
- ¹⁷ D. A. Demer and J. S. Renfree, "Variations in echosounder – transducer performance with water temperature", *ICES Journal of Marine Science*, **65**, 1021-1035 (2008).
- ¹⁸ "Section 7: Theory of operation", pp. 7-11, in *Operator manual: SIMRAD EK500 Fishery research echo sounder. Scientific echo sounder: Base version, P2170*. Simrad AS (now Kongsberg Maritime AS), Horten, Norway (1990-1997), 232 p.
- ¹⁹ R. J. Korneliussen, "Analysis and presentation of multifrequency echograms", Dr. Scient. thesis, University of Bergen, Department of Physics, Bergen, Norway (2002), 182 p.
- ²⁰ E. Ona, V. Mazauric and L. N. Andersen, "Calibration methods for two scientific multibeam systems", *ICES Journal of Marine Science* **66**, 1326-1334 (2009).
- ²¹ Ref. [3], pp. 180-182, 205, 220, and 225-235.
- ²² Ref. [4], pp. 350-361.
- ²³ This distinction is important to enable use of Eq. (31) in the integration over a multitude of scattering objects contained in a volume of finite extent, to derive the volume backscattering coefficient, cf. Section 3 and Eqs. (34)-(35).

- ²⁴ $\hat{\alpha} \equiv \alpha \cdot 20 \log_{10} e \approx 8.686\alpha$ is the absorption coefficient expressed in dB/m, where $e \approx 2.71828$ is Euler's number.
- ²⁵ L. L. Foldy and H. Primakoff, "A general theory of passive linear electroacoustic transducers and the electroacoustic reciprocity theorem. I", *J. Acoust. Soc. Am.* **17**(2) 109-120 (1945).
- ²⁶ L. E. Kinsler, A. R. Frey, A. B. Coppens and J. V. Sanders, *Fundamentals of acoustics*, 4th ed., J. Wiley & Sons, New York (2000), pp. 15, 189.
- ²⁷ "American National Standard. Procedures for calibration of underwater electroacoustic transducers", ANSI S1.20-1988 (ASA 75-1988), Acoustical Society of America, New York (2003). 40 p.
- ²⁸ Foldy and Primakoff [25] considered a lossless fluid medium, using time dependence $\exp(i\omega t)$, as here, and the lossless version of Eq. (22) was given, corresponding to $\alpha = 0$ (cf. their Eq. (50)). When repeating their derivation with fluid absorption accounted for, using a complex wavenumber $\kappa = k - i\alpha$ instead of the real wavenumber $k = \omega/c_0$ which was used by Foldy and Primakoff, Eq. (22) results.
- ²⁹ In acoustics, the concept "transducer gain" is analogous to the concept "antenna gain" or "power gain" used in electromagnetics [30], with similar definition and interpretation, cf. Eq. (24) and Section 6.3.
- ³⁰ C. A. Balanis, *Antenna theory: Analysis and design*, 3rd ed. J. Wiley & Sons, Hoboken, New Jersey (2005), 1117 p.
- ³¹ T. K. Stanton, "Multiple scattering with applications to fish-echo processing", *J. Acoust. Soc. Am.* **73**(4), 1164–1169 (1983).
- ³² K. G. Foote, "Correcting acoustic measurements of scatterer density for extinction", *J. Acoust. Soc. Am.* **88**(3), 1543–1546 (1990).
- ³³ X. Zhao and E. Ona, "Estimation and compensation models for the shadowing effect in dense fish aggregations", *ICES Journal of Marine Science* **60**, 155-163 (2005).
- ³⁴ K. G. Foote, "Linearity of fisheries acoustics, with addition theorems", *J. Acoust. Soc. Am.* **73**(6), 1932-1940 (1983).
- ³⁵ W. S. Burdic, *Underwater acoustic system analysis*, Prentice-Hall, New Jersey (1984), pp. 162-163.
- ³⁶ D. N. MacLennan, P. G. Fernandes, and J. Dalen, "A consistent approach to definitions and symbols in fisheries acoustics", *ICES Journal of Marine Science* **59**, 365-369 (2002).
- ³⁷ In the present theory, the range compensation becomes exact, $\bar{g} = 1$, and there is no TVG error. In general, some TVG error is likely in practice, as discussed by Foote *et al.* [9] and Simmonds and MacLennan [10], and \bar{g} should be accounted for as in Eq. (1).
- ³⁸ D. V. Holliday, "Extracting bio-physical information from the acoustic signature of marine organisms", In *Oceanic Sound Scattering Prediction*, N. R. Andersen and B. J. Zahuranec (eds.). Plenum Press, New York (1977), pp. 619-624.
- ³⁹ R. J. Korneliussen and E. Ona, "An operational system for processing and visualizing multi-frequency acoustic data", *ICES Journal of Marine Science*, **59**, 293-313 (2002).
- ⁴⁰ R. J. Korneliussen, "The acoustic identification of Atlantic mackerel", *ICES Journal of Marine Science*, **67**, 1749-1758 (2010).

APPENDIX A

Sonar equation for single-target backscattering

For reference, an interpretation of Eq. (13) in the form of a sonar equation is given in the following. Write Eq. (13) as

$$\frac{P_{bs}^{rms}}{P_{ref}} = \frac{P_{i,0}^{rms}}{P_{ref}} \cdot \frac{r_0}{r} \frac{r_0'}{r} \frac{r_1}{r_0'} \cdot |\mathbf{B}_i(\theta, \varphi)| \cdot e^{-\alpha(2r-r_0-r_0')} \cdot \frac{\sqrt{\sigma_{bs}}}{r_1} \cdot e^{-\alpha r_0'}, \quad (\text{A.1})$$

where $P_{i,0}^{rms} \equiv |\mathbf{P}_{i,0}|/\sqrt{2}$ and $P_{bs}^{rms} \equiv |\mathbf{P}_{bs}|/\sqrt{2}$ are effective pressure amplitudes, r_1 is a reference length (e.g. 1 m), and P_{ref} is an effective reference pressure (e.g. 1 μPa). Taking $20\log_{10}$ on both sides of Eq. (A.1) gives

$$EL = SL - TL_1 - TL_2 + BP + TS - 20\log_{10}\left(\frac{r_0'}{r_1}\right) - \hat{\alpha}r_0', \quad (\text{A.2})$$

which is the sonar equation for backscattering from a single target located on or off the acoustic axis in the far field of the transducer, at the angular frequency ω , under conditions of small-amplitude (linear) sound propagation.

Here $EL = 20\log_{10}(P_{bs}^{rms}/P_{ref})$ is the echo level, $SL = 20\log_{10}(P_{i,0}^{rms}/P_{ref})$ is the source level, $TL_1 = 20\log_{10}(r/r_0) + \hat{\alpha}(r-r_0)$ is the transmission loss for the field transmitted to the target, $TL_2 = 20\log_{10}(r/r_0') + \hat{\alpha}(r-r_0')$ is the transmission loss for the field backscattered from the target, $BP = 20\log_{10}|\mathbf{B}_i(\theta, \varphi)|$ is the beam pattern of the transmitted sound pressure field on decibel scale, and $TS = 10\log_{10}(\sigma_{bs}/r_1^2)$ is the target strength of the scattering object.

The latter two terms in Eq. (A.2) are required to account for absorption and spherical spreading over the distance from the scattering object to r_0' , since these are omitted from σ_{bs} (and thus TS), cf. Eq. (8). If absorption and spherical spreading were accounted for in σ_{bs} instead, these two terms would reduce to a single term, $-20\log_{10}(1/r_1)$.

APPENDIX B

Comparison with the Clay-Medwin acoustic power budget equations

Clay and Medwin [21] derived two alternative expressions of the “in-water” acoustic power budget equation for volume backscattering, given as (their Eqs. (7.3.10) and (7.3.17))

$$\langle p_e^2 \rangle = \begin{cases} N_f \langle \ell^2 \rangle \cdot \frac{r_0^2}{r^4} \cdot \frac{\Delta V_{eff}}{\tau_g} \cdot \int_0^{\tau_p} p_0^2(t) dt, & \tau_p \ll \tau_g \quad (\text{"short ping and long gate"}) \\ s_v \cdot \frac{r_0^2}{r^4} \cdot \Delta V_{eff} \cdot P_0^2, & \tau_p \gg \tau_g \quad (\text{"long ping and short gate"}) \end{cases} \quad (\text{B.1})$$

respectively, for the two cases of echosounder operation. Here, $\langle p_e^2 \rangle \equiv \frac{1}{\tau_g} \int_{t_{g1}}^{t_{g2}} p_e^2(t) dt$ is the “average echo squared” of the free-field backscattered sound pressure, in the fluid at the transducer front, accounting for the beam pattern of the receiving transducer. $p_0(t)$ is the sound pressure signal radiated by the transducer (the “ping”), at the range r_0 . For the case of “long ping and short gate”, $\tau_p \gg \tau_g$, $P_0^2 \approx \frac{1}{\tau_g} \int_{t_{g1}}^{t_{g2}} p_0^2(t - \frac{2r_i}{c_0}) dt = \frac{1}{\tau_g} \int_0^{\tau_g} p_0^2(t) dt$ is the average square amplitude of the ping. N_f is the number of targets per m^3 (target density), $\langle \ell^2 \rangle = \langle \sigma_{bs} \rangle$ is the expected value of the backscattering cross section of individual targets, and $N_f \langle \ell^2 \rangle = s_v$ is the volume backscattering coefficient. ΔV_{eff} is the effective sampled volume within the spherical shell gated volume V_g , given as $\Delta V_{eff} \approx r^2 dr \psi$ for large ranges relative to shell thickness, $r \gg dr$.

For the case of “short ping and long gate” ($\tau_p \ll \tau_g$) one may define $\langle p_0^2 \rangle \equiv \frac{1}{\tau_p} \int_0^{\tau_p} p_0^2(t) dt$. In this case one has $dr = \frac{1}{2} c_0 \tau_g$. For the case of “long ping and short gate” ($\tau_p \gg \tau_g$) one has $dr = \frac{1}{2} c_0 \tau_p$. By use of the expressions given above, Eqs. (B.1) may thus be written

$$s_v = \begin{cases} \frac{2r^2 \cdot \langle p_e^2 \rangle}{r_0^2 \cdot \psi \cdot c_0 \cdot \tau_p \cdot \langle p_0^2 \rangle} = \frac{2r^2 \cdot [tips]_{GV}}{r_0^2 \cdot \psi \cdot c_0 \cdot \tau_g \cdot [tips]_0}, & \tau_p \ll \tau_g \\ \frac{2r^2 \cdot \langle p_e^2 \rangle}{r_0^2 \cdot \psi \cdot c_0 \cdot \tau_p \cdot P_0^2} = \frac{2r^2 \cdot [tips]_{GV}}{r_0^2 \cdot \psi \cdot c_0 \cdot \tau_p \cdot [tips]_{0,GV}}, & \tau_p \gg \tau_g \end{cases} \quad (\text{B.2})$$

where the three “time-integral-pressure-squared” functions are defined as $[tips]_{GV} \equiv \int_{t_{g1}}^{t_{g2}} |p_e(t)|^2 dt$, $[tips]_0 \equiv \int_0^{\tau_p} |p_0(t)|^2 dt$ (for $\tau_p \ll \tau_g$), and $[tips]_{0,GV} \equiv \int_0^{\tau_g} |p_0(t)|^2 dt$ (for $\tau_p \gg \tau_g$).

A similar expression for the “in-water” acoustic power budget equation for volume backscattering, giving the volume backscattering coefficient, was derived by Medwin and Clay [22] for the case “short ping and long gate” ($\tau_p \ll \tau_g$), given as (their Eq. (9.3.17))

$$s_v = \frac{2r^2 \cdot e^{4\alpha r} \cdot [tips]_{GV}}{r_0^2 \cdot \psi \cdot c_0 \cdot \tau_g \cdot [tips]_0}, \quad \tau_p \ll \tau_g \quad (\text{"short ping and long gate"}). \quad (\text{B.3})$$

Eq. (B.3) extends the first of Eqs. (B.2) by accounting for sound absorption in the fluid, but otherwise the two expressions are equal.

To compare the theory presented here with Clay and Medwin’s [21] and Medwin and Clay’s [22] models, for evaluation of consistency, an “in-water” acoustic power budget equation may be derived from the theory given in the present work. From Eq. (13), which for the purpose of comparison is now extended to include the beam pattern of the receiving transducer (cf. the second of Eqs. (14)), so that the term $|\mathbf{B}_i(\theta, \varphi)|$ is replaced by $|\mathbf{B}_i(\theta, \varphi)|^2$, and by performing the same reasoning and volume integration as in Section 3.1, under the same assumptions, one finally obtains for the volume backscattering coefficient,

$$s_v = \frac{2r^2 \cdot e^{2\alpha(2r-r_0)} \cdot |\mathbf{P}_{bs}|^2}{r_0^2 \cdot \psi \cdot c_0 \cdot \tau_p \cdot |\mathbf{P}_{i,0}|^2}, \quad (\text{B.4})$$

which, in terms of echo integration formulation, for the two cases of echosounder operation, becomes (using a derivation procedure analogous to in Section 4)

$$s_v = \begin{cases} \frac{2r^2 \cdot e^{2\alpha(2r-r_0)} \cdot [tips]_{GV}}{r_0^2 \cdot \psi \cdot c_0 \cdot \tau_g \cdot [tips]_0}, & \tau_p \ll \tau_g \quad (\text{"short ping and long gate"}) \\ \frac{2r^2 \cdot e^{2\alpha(2r-r_0)} \cdot [tips]_{GV}}{r_0^2 \cdot \psi \cdot c_0 \cdot \tau_p \cdot [tips]_{0,GV}}, & \tau_p \gg \tau_g \quad (\text{"long ping and short gate"}) \end{cases} \quad (\text{B.5})$$

where $[tips]_{GV} \equiv \int_{t_{g1}}^{t_{g2}} |p_{bs}(t)|^2 dt$, $[tips]_0 \equiv \int_0^{\tau_p} |p_{i,0}(t)|^2 dt$ (for $\tau_p \ll \tau_g$), and $[tips]_{0,GV} \equiv \int_0^{\tau_g} |p_{i,0}(t)|^2 dt$ (for $\tau_p \gg \tau_g$).

Eq. (B.5) is the “in-water” acoustic power budget equation for volume backscattering from a thin spherical shell V_g (“gated volume”) of thickness $dr_g = \frac{1}{2}c_0\tau_g$ located in the far field of the transducer, under small-amplitude (linear) sound propagation conditions. It represents the analogue to the electroacoustic power budget equation, Eq. (38), for the case that only sound propagation in the fluid is considered, so that the transducer and electronics components of the echosounder system are not accounted for.

For each of the two echosounder operation cases, $\tau_p \ll \tau_g$ and $\tau_p \gg \tau_g$, the expressions given by Eqs. (B.2), (B.3) and (B.5) are equal, except for the fact that the derivation of Eqs. (B.2) was made for a lossless fluid medium ($\alpha = 0$), and that the absorption term related to r_0 is not accounted for in Eq. (B.3) (which in practice is of minor importance, since normally $r_0 \ll r$).

Retur: Havforskningsinstituttet, Postboks 1870 Nordnes, NO-5817 Bergen



HAVFORSKNINGSINSTITUTTET
Institute of Marine Research

Nordnesgaten 50 – Postboks 1870 Nordnes
NO-5817 Bergen
Tlf.: +47 55 23 85 00 – Faks: +47 55 23 85 31
E-post: post@imr.no

HAVFORSKNINGSINSTITUTTET
AVDELING TROMSØ

Sykehusveien 23, Postboks 6404
NO-9294 Tromsø
Tlf.: +47 77 60 97 00 – Faks: +47 77 60 97 01

HAVFORSKNINGSINSTITUTTET
FORSKNINGSSTASJONEN FLØDEVIGEN

Nye Flødevigveien 20
NO-4817 His
Tlf.: +47 37 05 90 00 – Faks: +47 37 05 90 01

HAVFORSKNINGSINSTITUTTET
FORSKNINGSSTASJONEN AUSTEVOLL

NO-5392 Storebø
Tlf.: +47 55 23 85 00 – Faks: +47 56 18 22 22

HAVFORSKNINGSINSTITUTTET
FORSKNINGSSTASJONEN MATRE

NO-5984 Matredal
Tlf.: +47 55 23 85 00 – Faks: +47 56 36 75 85

AVDELING FOR SAMFUNNSKONTAKT
OG KOMMUNIKASJON

Public Relations and Communication
Tlf.: +47 55 23 85 00 – Faks: +47 55 23 85 55
E-post: informasjonen@imr.no

www.imr.no

